THESIS FOR THE DEGREE OF LICENTIATE OF ENGINEERING

Thin-Film Electrocatalysts for Polymer Electrolyte Fuel Cells

Activity, Durability and Proton Conduction

Björn Wickman

CHALMERS

Department of Applied Physics
Chalmers University of Technology
Göteborg, Sweden 2007

Thin-Film Electrocatalysts for Polymer Electrolyte Fuel Cells
Activity, Durability and Proton Conduction
Björn Wickman

Department of Applied Physics
Competence Centre for Catalysis
Chalmers University of Technology
SE-412 96 Göteborg
Sweden
Telephone +46 (0)31 772 1000

Printed by:
Chalmers Reproservice
Göteborg, Sweden 2007

Thin-Film Electrocatalysts for Polymer Electrolyte Fuel Cells
Activity, Durability and Proton Conduction
Björn Wickman
Department of Applied Physics and Competence Centre for Catalysis
Chalmers University of Technology

Abstract

The polymer electrolyte membrane fuel cell (PEMFC) is a potential technology for future energy conversion in sustainable energy systems. By using hydrogen from renewable energy sources and oxygen from the air, the fuel cell produces electricity with water as the only exhaust. However, in order for fuel cells to be compatible with current techniques, several technological improvements are needed. The major issues are related to the platinum used to catalyze the oxygen reduction reaction on the cathode electrode, the proton conducting membrane and the durability of the fuel cell.

PEMFC electrodes typically consist of nanometer sized platinum electrocatalyst particles mixed with an ionomer and supported on carbon particles. The structural complexity of the electrode renders fundamental studies of its function difficult. Such studies are needed in order to increase the understanding and performance of the PEMFC electrode. For this purpose, model systems with well defined nanostructures should be used so as to isolate different governing mechanisms.

In this thesis, a structurally well controlled thin-film model system has been used to investigate PEMFC electrodes. The model electrodes were fabricated using thermal evaporation of the catalyst material directly on proton conducting membranes or gas diffusion layers. This procedure allows for short fabrication times, control over the amount of material deposited and a wide range of materials can be used. The samples were electrochemically evaluated in a conventional fuel cell under realistic operating conditions.

Evaluation of several different thin-film model systems demonstrated that the methodology can be used to qualitative compare and rank catalyst material in the PEMFC environment. Clear changes in the catalytic and structural properties of platinum were observed when the metal was mixed in bi-layers with iridium and titanium oxide. TiO_2 was found to operate as a proton conducting electrolyte in the PEMFC. In addition, adding TiO_2 between platinum and the carbon gas diffusion layer indicated an increased durability of the PEMFC electrode.

Keywords: fuel cell, PEMFC, model systems, cathode, oxygen reduction reaction, platinum, electrocatalyst, titanium oxide, Nafion, proton conduction, thin film evaporation

List of appended papers

Paper I:

Thin Film PtMe (Me=Au, Ir, TiO2) Catalysts for the Oxygen Reduction Reaction in the Polymer Electrolyte Fuel Cell
B. Wickman, H. Ekström, M. Gustavsson, L. Eurenius, G. Lindbergh, E. Olsson, B. Kasemo, and P. Hanarp
To be submitted to Journal of Power Sources

Paper II:

Nanometer-thick films of titanium oxide acting as electrolyte in the polymer electrolyte fuel cell
H. Ekström, B. Wickman, M. Gustavsson, P. Hanarp, L. Eurenius, E. Olsson, and G. Lindbergh
Electrochimica Acta 52 (2007) 4239-4245

Paper III:

Thin Film Electrocatalysts for PEM Fuel Cells
B. Wickman, H. Ekström, M. Gustavsson, G. Lindbergh and P. Hanarp
Conference Proceedings, Hydrogen and Fuel Cells 2007 International Conference and Trade Show (2007) 348-356

Table of Contents

1

Introduction

Since the industrialization, the world's energy consumption has constantly increased and during the 20^{th} century it has accelerated rapidly, with the growth of industrial production, transport, infrastructure and raised living standards. The growing need for energy is expected to continue in the future. With today's technology it will not be possible to provide enough energy if all countries would consume the same amounts of energy per capita as the western countries presently do.

Today, energy consumption relies strongly on the supply of fossil fuels, such as oil, coal and natural gas. As the amounts of fossil fuels are limited, this will emerge as a problem. Another important drawback of using the fossil fuels is the environmental problems that challenge the society in two ways: *i*) globally the release of carbon dioxide (CO_2) to the atmosphere increases the global warming which may change the climate on earth through the green house effect and *ii*) locally the burning of fossil fuels usually results in emissions of species such as nitrous oxides (NO_X), sulfur oxides (SO_X), hydrocarbons (HC) and particulate matter (soot), which are harmful for all living creatures [1].

The world is facing a serious energy and environmental challenge that has to be solved if the people of the world are to keep or increase their living standards, technical development and infrastructure. One way to continue economic growth and increased living standards for all is to find ways to use the limited energy resources more efficiently and in a more sustainable way. Fuel cell technology offers a more efficient energy usage than conventional technologies, such as combustion engines. The hydrogen (H_2), used as fuel, can be produced from renewable sources and the fuel cell will thus have little or no negative impact on the environment.

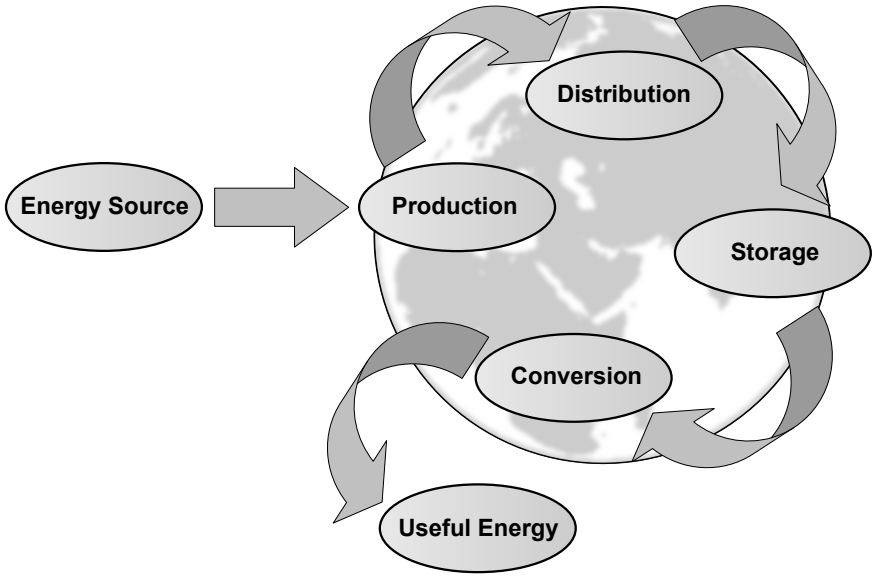

Figure 1.1: Schematic illustration of an energy system.

1.1 Energy challenge

The energy challenge is not a single problem, but related to the whole energy system with production, storage, distribution and conversion, see figure 1.1. A change from today's fossil fuel based system to a renewable system based on for example hydrogen will require a number of technological breakthroughs in the different areas.

1.1.1 Production

The majority of the energy consumed in the world is produced from non-renewable and finite sources such as oil, coal, natural gas and nuclear energy. In 2005, oil, coal and natural gas represented about 80 % of the total amount of energy consumed. Worldwide, oil is the most important energy carrier representing about 35 % of the world's energy consumption in 2005 while coal and natural gas covered 25 % and 21 % respectively [2]. Until now, the demand for more energy has been met by increasing the production of fossil fuel and, to some extent, controlled by the price. Some studies state that the fossil fuel resources will hit their peak production rate within the next

decades and increased production will be impossible. For oil production, it is likely that this peak will be met relatively soon which most likely will cause a rapid increase in the oil prices [3]. Increased prices will probably lead to a reduced usage of fuel, which can prolong the production time. When considering energy resources, it should also be noted that countries, such as Sweden, use much more energy than is produced within the country [4], and therefore strongly depend on other countries and are vulnerable for political changes.

The only long term sustainable option for energy production is to find ways of using renewable energy sources. In 2005 less the 13 % of the worlds energy consumption was produced from renewable sources [2]. The largest part of the renewable sources was the combustion of renewables, which contributed to 10 % of the energy consumption while hydro power supplied 2 %. Solar, wind and thermal together contributed only 0.5 %. Even if many of the renewable sources can be explored further to make a larger impact on the total energy consumption, it is critical that the world's total energy demand is decreased in order to produce enough energy in a sustainable way.

1.1.2 Storage and distribution

Energy is often used far away from the production sites and flexible use of energy is of great importance in today's society. Thus, there is a need to store and distribute fuel, from the sources to the consumers. In the fossil fuels, energy is stored chemically and can be used at need, e.g. when the engine in a car is turned on. Liquid fuels, such as gasoline, and solid fuels, such as coal, are easy to store and distribute and the infrastructure for doing this has been developed and refined for over a century. The losses involved in distributing solid and liquid fuels are low due to the high energy density of these fuels. Gaseous fuels such as natural gas or bio gas require compression of the gas in order to store and distribute them. This limits the distances over which the fuel can be distributed and puts high demands on the infrastructure. Electric power is not possible to store in large amounts but has to be used at the same rate as it is produced. It can however be converted to chemical energy, which for example is done in a battery or in the electrolysis of water to produce H_2.

1.1.3 Conversion

In the chain from energy source to energy use, the last step is conversion of stored energy into useful energy in the final application. For automotives, a

conventional combustion engine or an electrical engine can be used to produce mechanical energy to power the vehicle. In a combustion engine, the fuel is burnt to produce heat which is converted to mechanical energy. An electric engine needs electricity, either from a battery where energy is stored chemically or from a fuel cell producing electricity from the fuel.

1.2 Environmental challenge

1.2.1 Locally harmful emissions

Burning fossil fuels create a range of unwanted bi-products: *i*) impurities in the fuel, e.g. sulfur forms sulfur oxides (SO_X), *ii*) at high temperatures nitrogen and oxygen from the air forms nitrous oxides (NO_X) and *iii*) incomplete combustion leaves soot and hydrocarbons (HC) to be released to the atmosphere. The levels of locally harmful emissions can be brought down to acceptable levels, but these processes reduce the efficiency of the engine. Additionally, the release of CO_2 is difficult to reduce.

1.2.2 Global warming

Through the use of climate models and monitoring of the CO_2 levels in the earth's atmosphere it has convincingly been shown that human activities during the last 150 years is responsible for a major part of the increased global temperature, and that the temperature will increase significantly further if actions are not taken to decrease the CO_2 emissions. The only way to prevent further increase of the global temperature is to limit the use of fossil fuel and switch to renewable and sustainable energy sources [1].

1.3 Sustainable energy systems

The development of a new and sustainable energy system must take into account all steps in the energy chain: production, storage, distribution and conversion and their impact on environment and health. At the same time it must be feasible to adapt the infrastructure and to meet the energy demands throughout the world.

Using hydrogen, H_2 as energy carrier can in theory eliminate the use of fossil fuels. The H_2 can be produced from renewable sources such as water, wind and solar power. In the end, the H_2 can be converted into electrical energy through the use of fuel cells and used to power various electrical

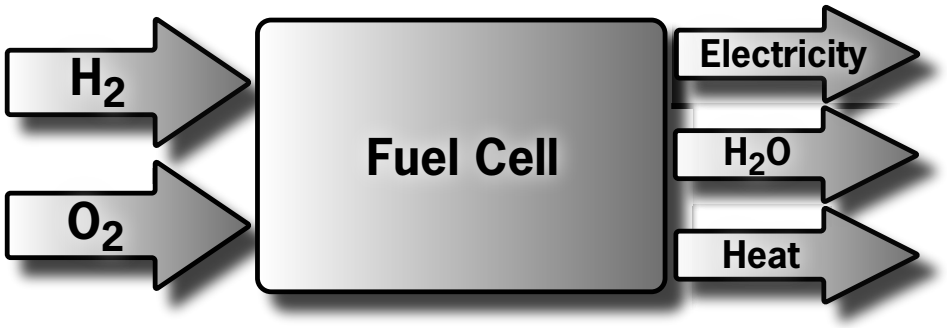

Figure 1.2: The general concept of the H_2-O_2 fuel cell.

devices, from small portable equipment up to electric cars and busses or even up to stationary power production.

1.4 Fuel cells

A fuel cell is a device that produces electricity as long as it is supplied with fuel. The simplest form converts H_2 and O_2 to water, electricity and heat, without pollutants and at high efficiency. Figure 1.2 shows schematically the concept of the H_2-O_2 fuel cell. The theoretical efficiency for converting chemical energy to electrical energy in a H_2-O_2 fuel cell is 83 % [5], which is much higher than conventional combustion engines, where the corresponding value is around 52 %. The principle of the fuel cell has been known since the mid 19^{th} century and during the past 20 years it has been intensively studied thanks to its potentially important role in a sustainable energy system.

Although the fuel cell is simple in principle, there are high demands on the fuel cell materials. The catalyst and electrode materials have to be stable in the highly corrosive environment and be able to convert H_2 and O_2 to H_2O fast and efficient at low temperatures. In addition, the fuel cell has to compete with current technologies for energy conversion, such as batteries and combustion engines.

Platinum (Pt) is the most commonly used catalyst material in low temperature fuel cells and contributes to a substantial part of the fuel cell production cost. Today's fuel cells require about 1 g of Pt per kW of energy produced and with a market price of Pt of about €30 $/g$ the Pt cost for a 100 kW fuel cell suitable for powering a car will be roughly €3000. To meet

the automotive cost requirements and make fuel cell cars compatible, the Pt content should be reduced to about 0.2 g/kW, hence a 5 time reduction of Pt metal in the electrodes [6]. This has to be done without decreasing the power density, i.e. the weight and size of the fuel cell should not increase appreciably. In addition, to meet the automotive requirements, the lifetime of a fuel cell, which today is around 2000 h of operation in a fuel cell car, has to be increased to about 5000 h [7].

The catalyst layer in the fuel cell consists of carbon particles forming a porous structure onto which Pt nanoparticles are deposited and mixed with a proton conducting polymer. Within the structurally and functionally complex layer reactants/products, electrons and protons are transported to and from the Pt catalyst particles. To be able to improve fuel cell electrodes with regard to activity and durability it is important to increase the understanding of the different processes involved and finding ways of studying them. By the use of model systems and simplified experiments it is possible to isolate structural or material parameters.

1.5 Motivation and objectives

In order to understand and improve fuel cell electrodes, I have in the work for this thesis, prepared nanometer thick catalyst layers and evaluated them in a real fuel cell under realistic fuel cell operating conditions. The thin films can be seen as being a thin slice of a real porous electrode, just at the interface between the membrane and the electrode. This model system has been used to evaluate the activity and stability of Pt in combination with other materials and to study proton transport in the electrode. Several material combinations and structures have been studied.

1.6 Outline of the thesis

This first chapter serves as a background of the energy and environmental challenges that are motivating the fuel cell research. In chapter 2 the theoretical background of the fundamentals of fuel cells, how they work and how they can be improved is discussed. Background to nanofabrication and model systems is given in chapter 3. Chapter 4, 5 and 6 deals with the work and the results of the thesis. Finally chapter 7 presents visions for future work.

2

Fuel cells

2.1 History

The Fuel cell is an old technology. Already in 1839 sir William Grove discovered and explained the fundamentals of the fuel cell. In Groves setup, two glass tubes, one filled with H_2 and the other with O_2, where placed in a beaker with acid electrolyte. In each of the glass tubes there was a Pt electrode in contact with the electrolyte and Grove was able to show a current flowing between the electrodes [5, 8].

More than one hundred years after the invention, General Electric developed and improved the fuel cell and in the early 1960s NASA used fuel cells in the Gemini space program. This was later followed by the Apollo program where fuel cells were used for electricity and water production in space [9].

In the 1970s the first car using fuel cells was built and since then the technology has been successively developed, and more passenger cars, buses, portable applications and stationary power production units with fuel cells have been demonstrated. Today the polymer electrolyte membrane fuel cell (PEMFC) using persulphonated fluoropolymers, such as Nafion (® DuPont), is the most promising technology for portable applications and transport. Many of the major car manufacturers have presented concept cars running on this type of fuel cell, such as for example the Honda FCX and the Mercedes A-Class F-Cell.

2.2 Principle

In ordinary combustion, on the atomic scale, the molecules of the fuel collide with oxygen molecules and react. The reaction takes place on the order of picoseconds and involves breaking of bonds in the fuel and formation of bonds between the fuel and the oxygen by redistribution of electronic charge.

The simplest example is burning of hydrogen:

$$H_2 + \tfrac{1}{2}O_2 \longrightarrow H_2O \tag{2.1}$$

As the reaction occurs, hydrogen-hydrogen and oxygen-oxygen bonds are broken, while hydrogen-oxygen bonds are formed. The enthalpy in the product, water, is lower than the combined enthalpy of the reactant hydrogen and oxygen, the reaction is exothermic. In ordinary combustion this energy difference is released as heat. The heat can subsequently be converted into mechanical energy which in turn can be converted to electric energy.

The principle of the fuel cell is to utilize the electrons when they move from/to the reactants and let them do work before they recombine and form the product. In a fuel cell, the energy difference can generate electricity directly from the chemical reaction. This is done by spatially separating the reactants (i.e. the H_2 and O_2) and forcing the electrons through an external circuit. The electrons generate an electric current as they move from the fuel to oxidant. A key element for achieving the spatial separation is the use of an electrolyte, a material that allows ions to flow but not electrons. On both sides of the electrolyte there have to be electrodes in direct contact with the electrolyte and connected through a circuit. The electrodes will harness electrons from the fuel on one side (anode) and distribute them on the oxidant side (cathode). Thus the overall oxidation of the fuel is split into two electrochemical half cell reactions. If we again look at the simple example of burning hydrogen, we have:

$$\text{Anode reaction:} \quad H_2 \longrightarrow 2\,H^+ + 2\,e^- \tag{2.2}$$

$$\text{Cathode reaction:} \quad \tfrac{1}{2}O_2 + 2\,H^+ + 2\,e^- \longrightarrow H_2O \tag{2.3}$$

The overall reaction is still the same as in ordinary combustion (reaction 2.1) but dividing the reactions and spatially separating them enables the fuel cell to generate electricity directly from the chemical reaction [10].

2.3 Choice of fuel and fuel cell

Above, the principle for the simplest fuel cell, the $H_2{-}O_2$ fuel cell is described. This fuel cell uses gaseous H_2 as fuel and protons (H^+) as charge carriers (i.e. protons diffuse through the electrolyte). This is the principle used in the polymer electrolyte membrane fuel cell (PEMFC), which is the fuel cell

type elaborated on in this thesis. There are, however, a number of other fuel cell types that differ mainly in their operating conditions, charge carrier and/or the type of electrolyte. Table 2.1 presents the most common types of fuel cells with typical applications along with their main advantages and weaknesses [5, 10].

The high temperature fuel cells (MCFC and SOFC) are mainly used in stationary power units where it is possible to use the high quality waste heat together with the produced electricity in a so called combined heat and power (CHP) system. At high temperatures, high reaction rates can be achieved without the use of expensive catalysts, but instead the high temperatures increase the demands on the materials used in the system and increase the start up time significantly.

Low temperature solid electrolyte fuel cells (PEMFC and DMFC) are well suited for transportation and portable electric applications. The use of liquid fuel in the DMFC makes the fuel handling relatively easy but on the other hand it has a considerably lower power density compared to the PEMFC.

2.4 Energy

The fuel cell produces electricity directly from a chemical reaction, and has a higher theoretic efficiency for conversion of the chemical energy to useful energy than a combustion engine. Thus, the fuel cell is a promising technology for energy conservation.

However, to compare the potential benefits of using fuel cells for energy conversion it is important to keep in mind the entire process of producing, distributing and storing the fuel before it is used in the fuel cell. As most fuel cells require H_2 as fuel and H_2 is not a natural resource such as oil, it has to be produced. Production of hydrogen can be made in three different ways: *i*) reformation of hydrocarbons such as fossil natural gas and petroleum or renewable biomass [11], *ii*) electrolysis of water [12] (this is basically a reversed fuel cell) or *iii*) photocatalysis to split water [13].

If H_2 is produced from fossil sources the production will lead to emissions of CO_2 in to the atmosphere and thus, some of the environmental benefits are lost. There are also practical problems with the high amounts of CO that is produced upon reforming. Most fuel cells are very sensitive to CO as it poisons the catalyst and extensive cleaning of CO has to be employed which reduces the efficiency. Different techniques, such as the water gas shift reaction can, however, be used to remove much of the CO [14].

Table 2.1: Key figures for different types of fuel cells (FC); Polymer electrolyte membrane (PEMFC), direct methanol (DMFC), phosphoric acid (PAFC), alkaline (AFC), molten carbonate (MCFC) and solid oxide (SOFC).

Fuel cell type	**PEMFC, DMFC**	**PAFC**	**AFC**	**MCFC**	**SOFC**
Electrolyte	Polymer membrane	H3PO4 (aq)	KOH (aq)	Molten carbonate	Ceramic, Yttria-Zirconia
Charge carrier	H^+	H^+	OH^-	CO_3^{2-}	O^{2-}
Fuel	H_2, Methanol	H_2	H_2	H_2, CH_4	H_2, CH_4, CO
Operating temperature (°C)	80-100	170-220	60-220	600-1000	600-1000
Power range (kW)	0.001-1000	10-1000	1-100	100-100000	10-100000
Catalyst	Pt	Pt	Pt	Ni	Ni
Advantages	- High power density - Good start/stop capabilities - Low temperature operations	- Low cost electrolyte - Reliable and long time performance	- Low cost materials - High performance	- High efficiency - Fuel flexibility - High quality waste heat	- High efficiency - Fuel flexibility - High quality waste heat
Weaknesses	- Expensive Pt catalyst - Sensitive to CO and S poisoning - Require water management	- Expensive Pt catalyst - Corrosive electrolyte - Require electrolyte management	- Expensive Pt catalyst - Require water management - Sensitive to CO_2	- Expensive materials - Corrosive electrolyte - Degradation and lifetime issues	- Expensive fabrication - Poor component stability
Applications	Electrical equipment, portable devices, transportation	Electrical equipment, transportation	Space, military	Stationary, electrical equipment	Stationary, transportation

Electrolysis of water to produce H_2 can be thought of as a way of storing electrical energy. If the electricity used is taken from renewable sources, this route produces H_2 without releasing harmful emissions or CO_2. Another possible advantage is that electricity is easily distributed using the electric grid and H_2 production can be done close to the usage sites, e.g. a filling station. The main disadvantage is that the extra conversion step of producing H_2 is accompanied by additional losses. Efficiency from electricity to compressed H_2 has been reported to vary between $60 - 90$ %, depending on production rate and delivery pressure [12].

For automotive use, studies of energy systems taking into account all steps in the energy production chain, so called well-to-wheel studies, point towards a possible total energy gain of using fuel cells or fuel cells combined with batteries, compared to other technologies [15]. Other studies recommend that batteries alone might be superior to fuel cells [16]. Creating an energy system based on fuel cells with little or no environmental impact throughout the energy chain is still a considerable challenge, but also a great possibility.

2.5 The polymer electrolyte fuel cell

The polymer electrolyte fuel cell (PEFC or PEMFC), also called proton exchange membrane fuel cell (PEMFC) or solid polymer fuel cell (SPFC) was developed in the early 1960s. The principle of the PEMFC is shown schematically in figure 2.1.

2.5.1 Fundamentals and components

This section describes the components that make up a typical PEMFC stack, explaining the fundamental role of each component and key parameters for their individual and combined performance.

The heart of the PEMFC is the membrane-electrode assembly (MEA), which is a three layer structure consisting of the polymer electrolyte and two electrodes. Figure 2.2 shows a photograph of a lab-scale MEA and an SEM micrograph of a cross section of an MEA. The electrodes contain an electrocatalyst layer and they are mounted on either side of the polymer membrane and form anode and cathode respectively. Optimizing the electrode structure is vital since the electrodes must facilitate transport of: *i*) ions to and from the membrane, *ii*) electrons to and from the current collectors and *iii*) product and reactants to and from the catalyst. A complete MEA is about $200 - 500$ μm thick and by the use of bipolar plates they can be stacked tightly to form a fuel cell stack. In the stack, the individual MEAs or cells

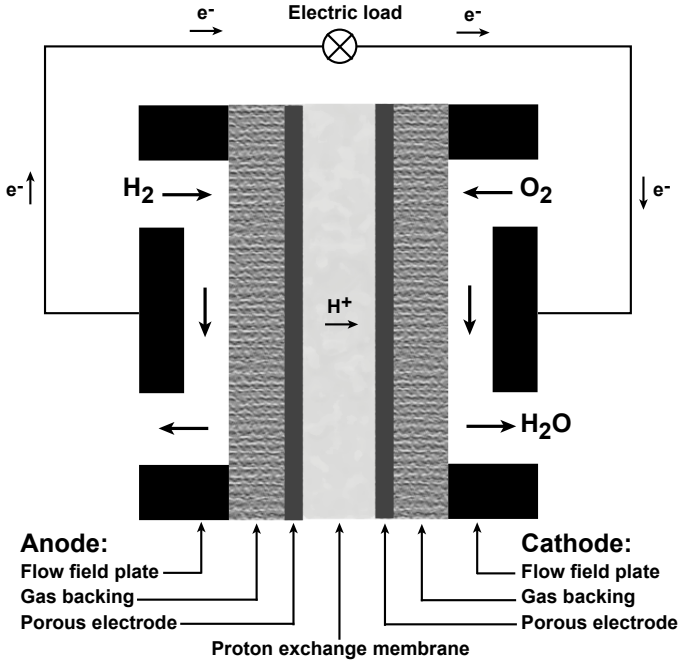

Figure 2.1: Schematic illustration of an operating PEMFC.

are connected in series and thus the total voltage from a stack is the voltage of each cell (about 0.7 V) multiplied by the number of cells. The total current is determined by the combined area of all cells in the stack [5].

i) Proton conducting membrane

The proton conducting membrane is a solid electrolyte that conducts protons from the anode to the cathode while it functions as an insulator for electrons. The thickness should be as small as possible in order to reduce the resistance of proton transport but must provide enough mechanical strength to keep the MEA together and be a seal between the reactant gases on either side. Typically, the thickness is $50 - 200\ \mu m$. Today, the most common proton conducting materials in the PEMFC are perfluorinated sulfonic acid polymers such as Nafion. Nafion consists of a polytetrafluoroethylene (PTFE, also known as Teflon) backbone grafted with fluorinated side chains terminated by sulfonic acid groups, HSO_3 [17]. The PTFE backbone is strongly hydrophobic while the sulfonic acid groups are strongly hydrophilic, i.e. readily attracts

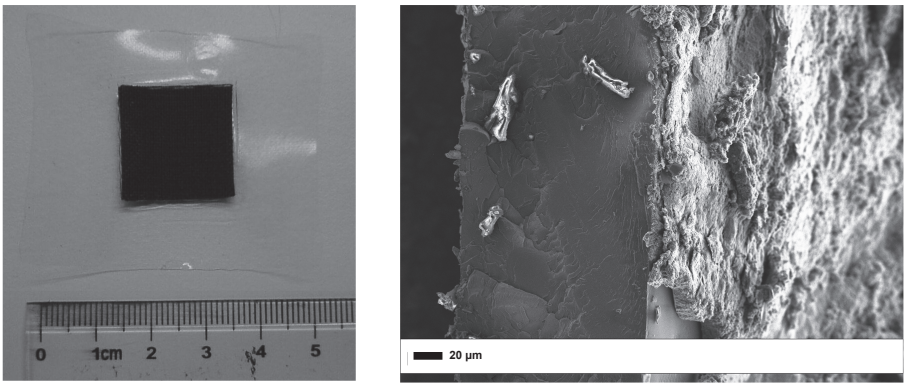

Figure 2.2: a) A photograph of a lab-scale MEA and b) an SEM cross section of an MEA.

water. In the hydrated regions the H^+ ions are loosely attracted to the SO_3^- and hence are able to move both inside the local water domain and between the water regions. A key factor for the proton conduction is the presence of water, as the membrane has to be hydrated. The proton conductivity drops drastically as the degree of hydration in the membrane is reduced. The need of hydrating the membranes poses challenges on the surrounding equipment as usually the gases entering the fuel cell need to be humidified. It also limits the operation temperature to below 100 ^oC. Besides being present in the membrane, the proton conducting polymer is also present in the electrode structure where it assures proton transport to the catalyst particles. It also acts as a binder and increase the mechanical stability of the electrode. The Nafion type materials are expensive to manufacture and since there is a need to raise the operating temperature towards 120 ^oC in order to increase the power generation of PEMFCs, research is dedicated to search for alternative proton conducting materials [18, 19].

ii) **Electrode**

The electrode or catalyst layer contains the electrocatalyst material. It must be an electric conductor and it should be prepared so that it can facilitate transport of ions, gases and water to and from the catalyst sites [20]. The most commonly used catalyst material is Pt and in the electrocatalyst layer it is present as highly dispersed nanoparticles to maximize the use of the

Pt. The electrode must have a high surface area and at the same time be chemically stable under voltage change in acidic conditions, i.e. high H^+ concentrations. Typically the electrode consists of carbon particles on the order of $50 - 100$ nm, Pt nanoparticles of $2 - 5$ nm and an ionomer binder that ensures proton transport and mechanical stability. On the anode side, the catalyst splits H_2 into protons and electrons and on the cathode side the catalyst adsorbs O_2 and catalyzes the oxygen reduction reaction (ORR). The electrodes are generally fabricated by printing, spraying or brushing an electrode ink, which is a suspension of catalyst powder in dilute ionomer solution and a solvent. The thickness of an electrode layer is usually $5 - 20$ μm.

iii) **Gas diffusion layer**

The gas diffusion layer (GDL) acts as a current collector, it distributes gases and prevents flooding of the electrodes. It is located between the electrodes and the bipolar plate. Usually it consists of a porous carbon fiber paper or woven cloth with a thickness of $100 - 300$ μm [20].

iv) **Bipolar plate**

The bipolar plates are cathode on one side in one cell and anode on the other side in the next cell. The plate gives mechanical stability to the stack, compresses and seals the cells and has groves for the reactant gases to be supplied. It is important that the plates have high electric and heat conductivity, that they are chemically stable and gas tight [21]. Ideally the bipolar plate should be as thin as possible to reduce electrical resistance and make the fuel cell stack small and light weight. However, this makes the gas channels narrow and increases the pressure drop over the plate and makes it difficult to pump gases. The result is that the bipolar plates actually comprise most of the stack volume and about 80 % of the weight. Issues in designing bipolar plates include: flow field patterns, material and manufacturing routines and cost. Typically bipolar plates are made by graphite or stainless steel.

v) **Surrounding system**

The surrounding system, also called balance of plant, includes management and control equipment to optimize the function of the fuel cell stack. The amounts and types of surrounding equipments depend on the size and type of stack, e.g. portable, transportation or stationary. For example, it is often attractive to operate large stacks (above 10 kW) at higher pressures which require a compressor, pressure regulators and possibly a turbine. Most fuel

cells use active water management to humidify the gases entering the stack to avoid membrane dehydration. It can also be of interest to hybridize the fuel cell stack with a battery which requires electric control systems. The stacks usually needs cooling and for small stacks it is often sufficient to use air cooling, possibly with fans or blowers while larger stacks often call for water cooling. The use of additional equipment can increase the efficiency of the fuel cell stack [22] but it adds to the system complexity and cost.

2.5.2 Benefits and problems

Fuel cells offer two important advantages as compared to current energy conversion technologies: *i*) high energy efficiency and *ii*) low and potentially zero environmental impacts. Fuel cells deliver energy as long as fuel is supplied and there is no need for recharging, there are no moving parts, they are silent and easy to mass produce.

The research during the past few decades have increased the performance and reduced the cost of fuel cells extensively. For example the Pt loading in the catalyst has been reduced from around $5 - 10$ mg/cm^2 in the early 1990s [23] to about 0.6 mg/cm^2 used today and at the same time the power density and life time have been increased. Many experts agree that continued research and optimization will continue to raise the performance of fuel cells and that the performance targets posted for large scale commercialization of fuel cells are feasible, for example, by using Pt alloys [6].

There are however several serious hurdles before fuel cells can be made commercially attractive. The major barrier is the cost involved in fuel cell systems, and not only the cost for the fuel cell and the fuel cell stack but also the cost of producing and distributing the H_2, i.e. massive changes in the infrastructure. The issues of lifetime and durability of fuel cells is also a considerable problem. Furthermore, power density, both of the fuel cell and the fuel, is a significant limitation. Fuel cells are also vulnerable to poisoning from e.g. CO and S, which puts additional constraints on the fuel. Also, the high price and limited resources of Pt is a problem for mass production of fuel cells.

Another problem is that the fuel cell technology is competing with already functioning and available technology. Thus, the fuel cells have to compete with conventional technology in terms of performance, cost and durability before it can be commercially attractive.

2.6 Electrochemistry

An electrochemical reaction involves transfer of charge, usually electrons between an electrode surface to an adjacent solution and is often termed electrode processes [10, 24]. In the simplest case this reaction occurs in three steps: *i*) adsorption of reactants at the liquid-solid interface, *ii*) electron transfer between the reactant and the electrode and finally *iii*) desorption of the products from the electrode surface. During electrochemical reactions, the electrodes will be charged, which gives rise to an electric double layer, a separation of negative and positive charges (ions) close to the electrodes [25]. This means a positively charged surface will have a layer of predominantly negatively charged ions in the electrolyte close to the surface and vice versa.

In fuel cells, a thermodynamically favorable process ($\Delta G < 0$, where ΔG is the change in Gibbs free energy) is used to generate an electric current. The amount of energy produced is dependent on the rate of the chemical reaction. Electrochemistry can also be used to drive thermodynamically unfavorable processes ($\Delta G > 0$), for example electrolysis of water, charging of batteries or electroplating. In this case, a current is supplied to the system and to some extent the rate of the chemical reaction induced can be controlled by the current, i.e. the rate of electrons passed.

Pt is not at all inert in the voltage window of an operating fuel cell and interactions with water induces chemical reactions on the Pt surface, something that is readily seen by performing cyclic voltammetry (CV) in inert atmosphere in a fuel cell, or in O_2-free electrolyte in a half cell. Figure 2.3 shows a CV for a polycrystalline Pt film in 0.5 M H_2SO_4 measured in an electrochemical quartz crystal microbalance (EQCM) cell at 18 ^oC. At potentials below 0.4 V vs. reversible hydrogen electrode (RHE) hydrogen adsorption and desorption peaks are seen, peak positions mainly depend on the governing crystal planes of Pt. In the forward scan, above 0.8 V vs. RHE Pt is oxidized and depending on sweep conditions, several different oxides may be produced [26]. On the reverse scan, the Pt oxide is reduced to metallic Pt.

2.7 PEMFC catalysis

A catalyst accelerates a chemical reaction. In heterogeneous catalysis this is done by adsorbing molecules from a gas or liquid phase on the catalyst surface where they react and the products desorb, leaving the catalyst unchanged. The catalyst increases the rate of a reaction by introducing new reaction paths or lowering of a rate limiting step, i.e. changing the kinetics, but

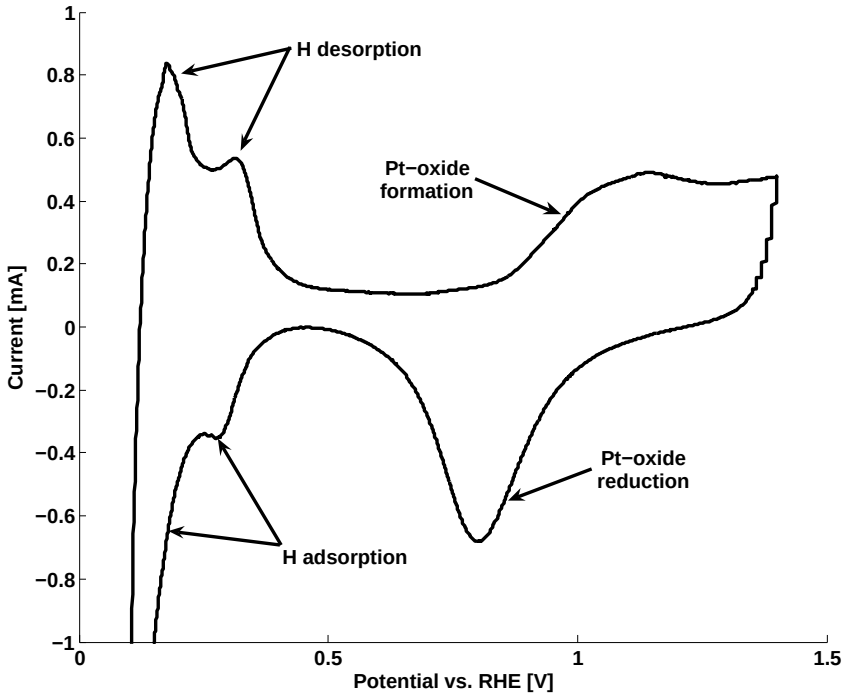

Figure 2.3: Cyclic voltammogram in 0.5 M H_2SO_4 for a polycrystalline Pt film at 18 ^oC measured in an EQCM cell.

not the thermodynamics of a chemical reaction. Catalysis involves three basic steps: *i*) bonding of molecules to the catalyst surface, *ii*) reaction on the surface and *iii*) separation of the formed product from the surface. If the second step is reaction between adsorbed species on the surface, it is called a Langmuir-Hinshelwood mechanism while if one of the reactants is taken directly from the gas or liquid face the mechanism is termed Eley-Rideal [27]. In addition to the three step process, a catalytic reaction usually involves diffusion of adsorbed species on the surface, multiple reaction paths and multiple reaction intermediates. It is sometimes sufficient to only study the overall or global reaction and derive the apparent reaction rates but in order to understand the fundamentals of a catalytic reaction, to be able to control and improve a process, e.g. selectivity and/or yield, it is necessary to study and understand the elementary reactions. As the rate of the overall reaction is limited by the rate of the slowest step in the reaction path (rate limiting step) a good catalyst must have a balance between binding energies

of reactants, intermediate complexes and products with activation barriers as low as possible.

In a fuel cell, electrode processes and catalysis work simultaneously in electrocatalysis, and it is important to understand the underlying processes and how they interact. For a fuel cell to deliver energy the chemical reactions have to occur at a high rate and a catalyst is employed to do this. However, in variance with traditional heterogeneous catalysis, the processes take place in the presence of a potential. A change in potential is similar to a temperature or pressure change in regular catalysis. This is evident from the definition of change in Gibbs free energy:

$$dG = -SdT + Vdp - dW_{elec} \tag{2.4}$$

Which is derived from the first and second law of thermodynamics [10]. The term dW_{elec} is the electric work, defined as the work done by moving a charge Q_c through an electric potential E:

$$W_{elec} = Q_c E \tag{2.5}$$

If the charge is carried by electrons:

$$Q_c = nF \tag{2.6}$$

Where n is the number of moles of electrons transferred and F is Faradays constant. Thus, the driving force of chemical reactions, dG is changed when the potential in the fuel cell is changed. This means that reactions can be increased (or suppressed) by a change in potential. In a fuel cell under operation, the potential will change due to the load and it is important to understand how this affects the chemical reactions and the performance of the cell.

2.8 PEMFC performance

The combined losses in the fuel cell system can be expressed as an efficiency which relates the amount of energy put into the system to the amount of useful energy taken out of it. Additionally, durability of the system and its components is crucial in order to sustain the performance of the fuel cell over time. Below, these terms will be explained in more detail.

2.8.1 Thermodynamics

The theory of thermodynamics is used to describe and track properties of a system in terms of energy and entropy. The first law of thermodynamics says that energy can never be created nor destroyed while the second law says that the entropy of a system and its surroundings must increase or at least remain zero for any process [10]:

$$1^{st} \text{ law of thermodynamics:} \quad dU = DQ - dW \tag{2.7}$$
$$2^{nd} \text{ law of thermodynamics:} \quad dS_{univ} \geq 0 \tag{2.8}$$

Where U is the internal energy of a closed system, Q is heat, W is work and S is the entropy.

The most important thermodynamical quantities when considering chemical reactions are enthalpy, H, and Gibbs free energy, G.

$$G = H - TS \tag{2.9}$$

Equation 2.4 relates the change in Gibbs free energy to changes in temperature, pressure and electric potential. For a constant temperature, constant pressure process and using molar quantities for a reaction, this reduces to:

$$\Delta\hat{g}_{rxn} = -nFE \tag{2.10}$$

Considering the PEMFC reaction, i.e. H_2 and O_2 forming water:

$$H_2 + \tfrac{1}{2}O_2 \longrightarrow H_2O \tag{2.11}$$

This reaction has $\Delta\hat{g}^0_{rxn} = -237.17\ kJ/mol$ at standard state conditions ($T = 25\ ^oC$ and $P = 1\ bar$). Thus the reversible voltage for a $H_2{-}O_2$ fuel cell operating at standard conditions is:

$$E^0 = \frac{\Delta\hat{g}^0_{rxn}}{nF} = 1.23\ V \tag{2.12}$$

This is the theoretical upper limit of the reversible potential in a PEMFC at standard state conditions. The term reversible voltage implies that the system is at equilibrium, thus equation 2.12 will not be valid as current is taken from the cell and the cell voltage will always be lower than E^0.

Thermodynamics can also be used to determine the ideal reversible fuel cell efficiency. Efficiency, ε can be defined as:

$$\varepsilon = \frac{what\ you\ get}{what\ you\ pay\ for} \tag{2.13}$$

Which means how much useful energy can be extracted divided by the total amount of energy put into the system. Equation 2.4 says that the maximum amount of energy available to do work is the Gibbs free energy of the reaction and the total amount of energy released in the reaction is the enthalpy, and thus:

$$\varepsilon_{FC} = \frac{\Delta\hat{g}}{\Delta\hat{h}} \tag{2.14}$$

At room temperature and atmospheric pressure this yields [5]:

$$\varepsilon_{FC} = \frac{\Delta\hat{g}^0}{\Delta\hat{h}^0} = 0.83 \tag{2.15}$$

Thus, the maximum electrical efficiency for the PEMFC at room temperature is 83 % (the remaining is converted to heat). This can be compared to the theoretical efficiency of a combustion engine which is restricted by the Carnot cycle:

$$\varepsilon_{Carnot} = \frac{T_O - T_R}{T_O} \tag{2.16}$$

An engine with an operating temperature (T_O) of 400 ^oC and rejection temperature (T_R) at 50 ^oC will thus have a theoretical reversible efficiency of 52 %.

2.8.2 Kinetics

In ordinary chemical reactions, electrons are transferred between the reacting species directly, without the liberation of free electrons, while for electrochemical reactions electrons are transferred between electrodes and the reacting species. This means that there is always a current present as reactions take place and the current can be related to the rate of the reaction. Consider again the over all reaction in the PEMFC:

$$\mathrm{H_2} + \tfrac{1}{2}\mathrm{O_2} \underset{k_b}{\overset{k_f}{\rightleftharpoons}} \mathrm{H_2O} \tag{2.17}$$

k_f and k_b are the rate constants for the forward and backwards reaction respectively, and from classical kinetic theory it is possible to derive expressions for the reaction rates. The reaction rate ν, depends on reactant concentration C, the rate constant k, the activation barrier $\Delta G^{\ddagger}$ and temperature T. The net reaction rate may be written as:

$$\nu = \nu_f - \nu_b = k_f C_R^* e^{\left(-\frac{\Delta G_f^{\ddagger}}{RT}\right)} - k_b C_P^* e^{\left(-\frac{\Delta G_b^{\ddagger}}{RT}\right)} \tag{2.18}$$

Where R is the gas constant, subscripts R and P represents reactants and products respectively in the net reaction (products in the forward reaction is reactants in the backwards). Superscripts $*$ are used to highlight the fact that for the fuel cell reaction, the products and reactants are absorbed species on the catalyst surface. The reaction rate can be related to the measurable exchange current density j, as current is nothing more than a rate of electrons. Here, it is the rate at which electrons are released in the chemical reaction, and thus:

$$j = j_f - j_b = nF\left(\nu_f - \nu_b\right) \tag{2.19}$$

At thermodynamic equilibrium there is no net reaction and thus no net current is measured ($j = 0$). In other words:

$$j_f = j_b = j_0 \tag{2.20}$$

j_0 is termed the exchange current density of the reaction and is a critical parameter for the fuel cell performance.

As the potential in an electrochemical system is changed from equilibrium, the activation energy barriers are changed. The forward and backward energy barriers are related to the Gibbs free energy of the reaction, as:

$$\Delta G_{rxn} = \Delta G_f^{\ddagger} - \Delta G_b^{\ddagger} \tag{2.21}$$

The potential difference $(E^0 - E)$ is defined as the overpotential, η and represents the losses in the system. The magnitude of η is simply the difference between the equilibrium potential and the actual value. To relate a change in potential to the change in activation barrier, a term called transfer coefficient, α is introduced. The value of α represents the symmetry of the

activation barrier and for a symmetric reaction the value is 0.5. A change in potential to a more positive value lowers the energy of the reactant electron. The activation barrier of the oxidation (backward reaction, $\Delta G_b^{\ddagger}$) is lowered by a fraction of $(1-\alpha)\,F\eta$, while the reduction reaction (forward reaction, $\Delta G_f^{\ddagger}$) is increased by a fraction of $\alpha F\eta$.

This makes it possible to express the potential dependence of the current density and this is described by the Butler-Volmer equation:

$$j = j_f - j_b = j_0 \left(e^{\left(\frac{\alpha n F \eta}{RT}\right)} - e^{\left(-\frac{(1-\alpha) n F \eta}{RT}\right)} \right) \tag{2.22}$$

The Butler-Volmer equation describes how current and voltage are related in an electrochemical system, and in equation 2.22 it assumes that the concentrations of reactant and products on the surface are unaffected by the net reaction. It can be seen that the current produced by the electrochemical reaction increases exponentially with overpotential and that an increase in current results in a loss of voltage (activation loss, η_{act}).

From equation 2.22 it is seen that for large η the second term becomes negligible and thus:

$$j = j_f - j_b = j_0 e^{\left(\frac{\alpha n F \eta}{RT}\right)} \tag{2.23}$$

Solving for η yields:

$$\eta = -\left(\frac{RT}{\alpha n F}\right) \ln j_0 + \left(\frac{RT}{\alpha n F}\right) \ln j \tag{2.24}$$

A plot of η versus $\ln j$ will thus produce a straight line and is often presented as the Tafel equation:

$$\eta = a + b\, \ln j \tag{2.25}$$

Where a and b are constants and b is called the Tafel slope. Another common way to write the Tafel equation highlights the importance of the exchange current density, j_0:

$$\eta = b\, \ln \frac{j}{j_0} \tag{2.26}$$

The performance of the fuel cell depends on the operating conditions, pressure and gas concentrations. The E^0 value calculated above is the equilibrium

potential at standard conditions and assumes 100 % H_2 and O_2. The equilibrium potential of a fuel cell running at different conditions is described by the Nernst equation [10]:

$$E_{eq} = E^0 + \frac{RT}{nF} \ln \frac{P_{H_2} P_{O_2}^{1/2}}{P_{H_2O}} \tag{2.27}$$

The PEMFC half cell reactions look fairly simple but they involve several intermediate steps and at different potentials there are several possible side reactions that may occur. Most problems arise at the cathode side where O_2 is reduced to H_2O. For a single O_2 molecule reaction 2.3 becomes:

$$O_2 + 4\,H^+ + 4\,e^- \longrightarrow 2\,H_2O \tag{2.28}$$

This reaction is termed the oxygen reduction reaction (ORR) and is a four-electron reaction, including the transfer of four protons and the cleavage of an O−O bond. The incomplete two-electron reduction results in formation of hydrogen peroxide (H_2O_2). Two different reaction mechanisms have been proposed for the ORR reaction, *i*) the simple dissociative mechanism where the O_2 is split on the catalyst surface and *ii*) the associative mechanism where O_2 does not dissociate on the surface. Nørskov *et al.* [28] have presented a method to use density functional theory (DFT) to estimate the thermochemistry for electrochemical reactions and found that the binding energy of O and OH to the catalyst surface are key parameters for the ORR reaction. Further, it was concluded that no sole material has higher activity for the ORR than Pt, but that it should be possible to raise the activity by changing the electronic properties of Pt, e.g. by alloying.

2.8.3 Transport of species

In order for the fuel cell reaction to occur, the transport of *i*) reactant and product species (mass transport) to and from the catalyst sites and transport of *ii*) electrons and protons (charge transport) between the electrodes has to be as efficient as possible.

i) Mass transport

Mass transport occurs via diffusion and/or convection. Convection refers to transport of a species under the action of mechanical forces, e.g. the motion of a fluid or gas, while diffusion refers to a transport of species due to concentration gradients. Diffusion is restricted by the molecular motion, depending

on the temperature and the dimensions of the space where diffusion takes place. It is thus far less effective than the convectional transport which is related to the mechanical force applied, e.g. the flow rate of the gas.

In the fuel cell, reactant gases are supplied through the gas channels in the bipolar plates and the gas has to diffuse through the gas diffusion layer to reach the active catalyst sites. At high current densities, gases have to be supplied at high rates to the cell. However, at some level the diffusion will not be sufficient and the performance of the fuel cell will radically decrease with increasing current. This is termed mass transport losses (η_{trans}) or Nernstian losses since they can be modeled by the Nernst equation (equation 2.27). To minimize this effect, the distance where gases have to be transported through diffusion should be made as small as possible.

ii) **Charge transport**

Charge is transported in the fuel cell via electrons moving in the outer circuit and via protons moving through the electrolyte. The transfer of electrons is rarely a big issue in fuel cell design, the electrode, the gas diffusion layer and the bipolar plates are good electric conductors and the losses associated with electron transfer are very small.

Proton transport however, is far more difficult than electron transfer, mainly due to the large difference in mass. In general, proton conductivity in solid materials is far below the upper limit for proton conduction in liquids. However, proton conducting polymers such as Nafion shows conductivities close to that of liquid systems as a consequence of the combination of hydrophobic and hydrophilic groups present in the structure [17]. This leads to a system where water can easily move and the conductivity is essentially carried by hydrated protons, e.g. H_3O^+ and governed by the diffusion coefficient of water.

Resistance to charge transport results in a voltage loss in the fuel cell. The losses obey Ohms law, and are therefore termed ohmic losses (η_{ohm}) or IR losses. To minimize the ohmic losses the membrane should be as thin as possible. However, if the membrane is too thin, H_2 and/or O_2 will diffuse through the membrane and react, meaning that fuel is basically lost. Also, a thin membrane increases the amount of electrons transported through the membrane and energy is lost as the fuel cell is short circuited. These two effects results in a voltage loss termed fuel crossover losses (η_{cross}) or internal current losses. The fuel crossover losses are often combined with the activation losses when the fuel cell performance is analyzed.

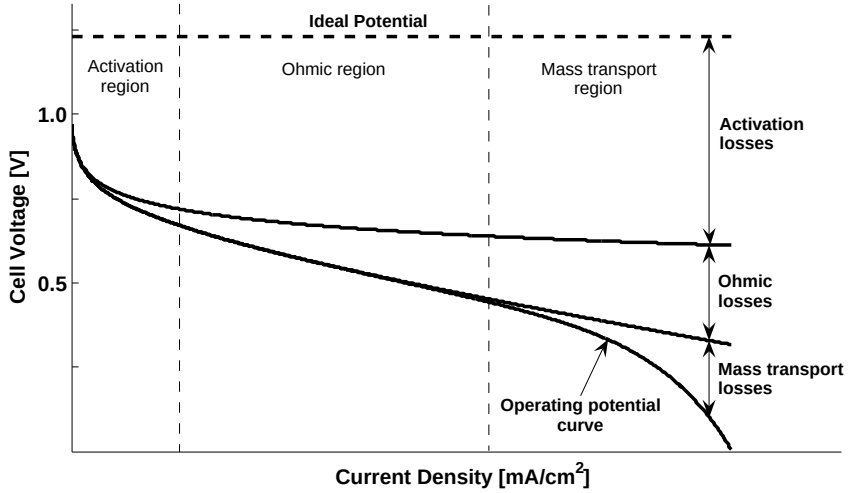

Figure 2.4: Schematic illustration of the operating potential curve, with the contributions from the different potential losses and the different polarization regions.

2.8.4 Losses

Kinetics and transport of species in the fuel cell results in three types of irreversible losses: *i*) Activation losses, *ii*) ohmic losses and *iii*) mass transport losses. These losses can be expressed as voltage drop or overpotential and will add together to give the total overpotential for the fuel cell. The resulting potential is thus:

$$E = E_{eq} - \sum \eta = E_{eq} - \eta_{act} - \eta_{ohm} - \eta_{trans} \tag{2.29}$$

Figure 2.4 shows a schematic illustration of the resulting fuel cell operating potential curve where the contributions from the different potential losses are seen.

2.8.5 Efficiency

The losses described above will lead to a reduced voltage in the cell. These are unwanted losses, and the efficiency will be lower than the theoretical efficiency calculated in equation 2.15. As seen in figure 2.4 the fuel cell potential varies with current, thus the efficiency will vary with current. A typical fuel

cell normally operates at about 0.7 V, the ideal voltage is 1.23 V (at room temperature) and the efficiency of the cell is thus:

$$\varepsilon = \frac{E}{E^0}\frac{\Delta\hat{g}^0}{\Delta\hat{h}^0} = 0.47 \tag{2.30}$$

The actual efficiency from fuel to electric energy is here only 47 %, quite far from the 83 % that is theoretically possible.

2.8.6 Stability

In order for fuel cells to become a realistic alternative for energy conversion, they must not only have a high performance, they must also be able to keep the performance over time. The US Department of Energy has defined the target lifetime of an automotive fuel cell stack to 5000 h (equivalent to about 240 000 km) for the year 2010 [7]. In 2005 this number was about 2000 h [29]. All parts of the fuel cell are subjected to degradation and usually a failure in one component results in failure of the whole fuel cell. The most critical components are the electrodes (mainly the cathode electrode) and the membrane.

Degradation of a Pt/C electrode is associated with three fundamentally different processes: *i*) coalescence of Pt nanoparticles via Pt particle migration on the support, *ii*) Pt dissolution and redeposition (an Oswald ripening process) and *iii*) loss of Pt particles due to corrosion of the support [30, 31]. Moreover, Pt has been found to migrate into the polymer membrane during voltage cycling [32]. All these processes are strongly dependent on operating conditions, such as cathode potential, relative humidity, scan rate and temperature. For the third point, it has been suggested that Pt can catalyze carbon corrosion [33, 34]. Other studies have, however, reported that Pt on the carbon do not significantly increase the rate of carbon corrosion [35]. It is often observed that the Pt particles in the cathode catalyst increase in size after fuel cell operation, a result of point one and two above, but there is little evidence to which of the two mechanisms that dominate. Pt dissolution is dependent on potential and rate of potential change in acidic media, and it has been suggested that oxidized Pt is more subjected to diffusion than Pt metal [36]. Moreover, it has been proposed that the stability of Pt can be improved by alloying with transition metals such as Cr, Ni or Co [37].

Also the polymer membrane suffers from aging effects and loses performance over time in the fuel cell. Issues related with membrane degradation are: *i*) chemical degradation, *ii*) poisoning effects and *iii*) mechanical degradation [38].

2.9 Improving fuel cell catalysts

In one way or another, improving fuel cell catalysts usually means to raise the amount of power with respect to system cost (initial and running). Different applications put different limits on features such as size, weight or lifetime and the routes for improvement may differ depending on the type of application. However, for all systems it is desirable to have a reliable, stable operation, high power density and a low system cost. For the catalyst, this means that several properties might need improvement, e.g. activity, durability, poison resistance, active surface area, conductivity and catalyst utilization. Improvements can be achieved by optimizing the catalyst layer composition, electrode design, employment of new materials or material combinations and control of the operating conditions.

2.9.1 Structure

The structure of the electrode, both on micro and macro level and parameters like porosity, electrode thickness, ionic and electric conduction, distribution and size of the catalyst particles can have significant impact on the fuel cell performance. The internal volume should be large in order give a high surface area of the catalyst, but the overall volume of the electrode should be small enough to reduce mass transport and size. The catalyst layer should create the same environment for all catalyst particles, enabling high utilization. Studies have shown possible effects of introducing ordered structures in the electrode, such as carbon nanotubes [39] and nanowhiskers [40, 41].

Changing the particle size of the catalyst will affect the activity for the ORR. It has been shown that the mass activity of Pt particles has a maximum around 3.5 nm while the specific activity (surface activity) increase with particle size [42]. However, to increase the surface area of the catalyst, particles are made small, usually around $2 - 5$ nm.

2.9.2 Composition

Optimizing the electrode composition and the composition of the catalyst has shown to have a major impact on improving fuel cell catalysts. Changing the composition of the catalyst material, e.g. via alloying or deposition of nanoparticles on different support materials can affect the catalyst activity in two ways: *i*) by spillover mechanisms and/or *ii*) electronic modifications. Introducing new materials in or close to the catalyst can also influence the stability of the electrode [37].

2.9.3 Operating conditions

Fuel cell efficiency depends on the operating voltage/current and it has been shown that durability is more dependent on potential cycling and the potential limits than time of operation [43]. For example, accelerated aging is usually achieved by excessive cycling. Also the stability of both carbon and Pt in acidic media is dependent on potential and operating environment [36]. To increase the lifetime of fuel cell stacks it is common to employ an electric control system to avoid open circuit potential (OCP). The power needed from a fuel cell is far from constant with respect to time. For example, a car requires a lot of energy for acceleration under short times while it uses only a portion of this when driving at a constant speed. In order to handle the peak power demands, the system has to be over dimensioned. A possible way to both create a stable performance for the fuel cell and at the same time reduce the system size is to hybridize the fuel cell. This is done by incorporating a battery that can provide additional power at peak loads and that can be charged by the fuel cell at low loads. In this setup it is also possible to use break energy to charge the battery which further reduces the size of the fuel cell.

3

Nanofabrication of model catalysts

Fuel cell electrodes have a complex structure and there are a large number of chemical reactions and processes occurring simultaneously and affecting each other. In studies on real fuel cell electrodes, it is often difficult to separate different mechanisms that influence the result. To solve this black box problem, it is often necessary to make simplified experiments using model systems. Since the active catalyst particles in a real fuel cell are on the nanometer range, controlled nanofabrication methods can be used for model catalyst fabrication.

3.1 Nanofabrication - dimension and control

In a nanomaterial, at least one of the material dimensions is on the nanometer scale (larger than 1 nm and much smaller than 1 μm). A 1 nm ($= 10^{-9}$ m) thick film of a material like Pt, which has an FCC structure and a lattice constant of 3.92 Å, is equivalent to about 5 atomic layers. Consequently every fifth atom is located on the surface, which means that the ratio between surface and bulk atoms is large. In addition, thin films typically are not continuous but form clusters, thus further increasing the fraction of surface atoms for a nanomaterial. Many of the processes that occur in materials have relevant length scales on the orders of nanometers and when the material dimensions are close to these, the material properties will differ compared to bulk material [44].

There are many different techniques to fabricate nanostructures, for example lithography routines (such as electron beam, colloidal and photo lithography), stamping techniques and chemical and physical preparation (microemulsions, thin films etc.). A review of nanofabrication techniques can be found in [45]. The different techniques offer different possibilities for the

fabrication procedure regarding parameters such as, *i*) size of the structures that can be fabricated, *ii*) sample area that can be covered, *iii*) time of preparation and *iv*) quality and control of the resulting nanostructure.

3.2 Model system approach

Compared to a real system, a model system is more defined, with high control over important parameters such as, particle size, inter particle separation, amount of material or materials and support material. Various model systems have efficiently been used in heterogeneous catalysis [46]. When simplifying a system in order to isolate specific mechanisms, it is important to keep in mind that several processes that occur in the real system are eliminated. The combined effects of different processes may not be seen and it is possible that new phenomena are introduced in the model systems that do not exist in the real system. The results from the model studies usually need to be translated to the real system, which is often not straightforward. In most cases there is a trade off between how realistic the model system is and how well controlled it is.

3.3 Model systems for fuel cells evaluated in the real fuel cell environment

There are typically two ways in which new catalyst materials for fuel cells are tested. The first is it to synthesize a new catalyst material, deposit it on to porous carbon and create an electrode which is then tested in a fuel cell [37]. The second way is to prepare a model system on a flat substrate and evaluate it in a half cell setup using for example rotating disc electrode [47]. An alternative approach [48, 49, 50], takes advantages from both routes above. The system, termed thin-film catalysts, is the model system used in this work. The approach is to fabricate nanometer thick catalyst films on membranes or gas diffusion layers (GDL) and test them in a single cell fuel cell. This model system, which is relatively fast end easy to fabricate, can at the same time be evaluated under realistic conditions in a real fuel cell. Figure 3.1 shows schematically the principle of the thin-film catalyst model system. The idea is that the catalyst films deposited on either the membrane or the GDL essentially mimic a thin slice of a real electrode, in the interface between the membrane and the GDL.

The main advantage with the thin-film model system is that the catalysts can be evaluated under realistic fuel cell conditions. Thus, most of the

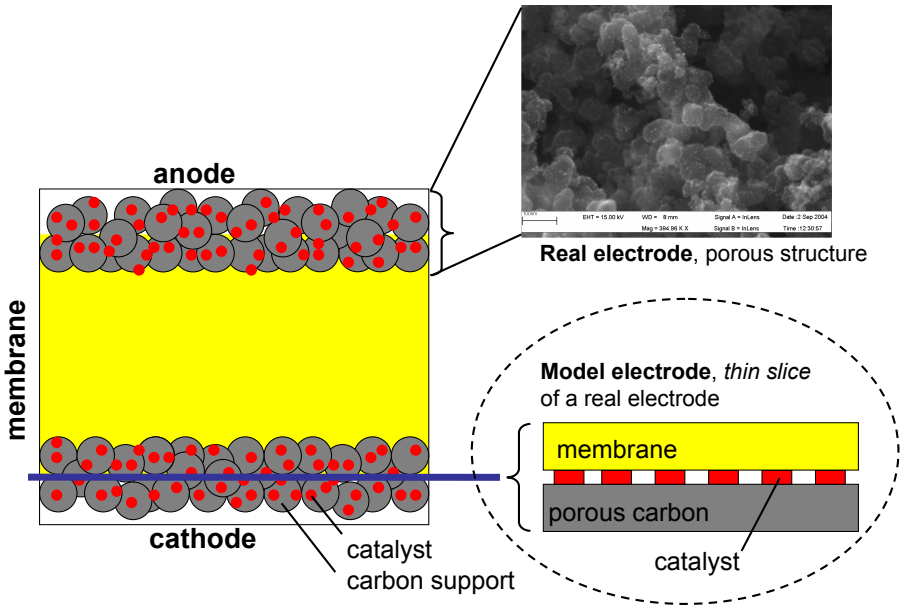

Figure 3.1: Schematic illustration of the thin-film model system.

processes occurring in a real electrocatalyst layer are accounted for. The model system is fairly well controlled and possible to characterize both using physical methods and electrochemical methods.

4

Objectives of this thesis

The main objectives in this thesis have been to develop a thin-film catalyst model system and to explore the possibility to study the model electrocatalysts under realistic fuel cell conditions. The work has been focused on fundamental physical processes in order to identify key factors that may improve state of the art PEMFCs. To achieve this, thin film nanofabrication and characterization methods have been combined with sensitive state of the art single cell fuel cell tests. By depositing nanometer thick layers of catalyst materials, with high control over the amount of material deposited and the ability to characterize the resulting structures both physically and electrochemically, it is possible to compare catalyst formulations with respect to activity, stability and selectivity. The work has been focused on improving the catalyst activity and durability at the cathode.

5

Sample fabrication and characterization

In this chapter, the nanofabrication procedures and main characterization methods used in this work are discussed.

5.1 Nanofabrication of thin-film catalysts

In paper I and II, nanometer thick films of Pt and Pt in combination with other materials where deposited directly onto Nafion membranes. In paper III the same deposition technique was used but the substrate was changed to a gas diffusion layer. The thin film deposition was done using thermal (electron-beam) evaporation in vacuum (AVAC HVC-600, 10^{-6} $mbar$). A schematic description of the evaporation procedure is shown in figure 5.1.

The principle of the deposition technique, in the present case, is that an energetic electron beam is directed onto the source material, intended for deposition. The kinetic energy of the impinging electrons is converted into heat upon hitting the source and at a sufficient rate of energy deposition the source will melt and material evaporate onto the surrounding surfaces. A substrate placed on one of the surrounding surfaces and is thus covered with the source material.

A quartz crystal microbalance (QCM), situated in the vacuum chamber is used to carefully measure the thickness of deposited material. For the samples fabricated in this work, the typical deposition rate was about 1 Å/s.

Thermal evaporation can be used to deposit a wide range of materials and it is possible to sequentially deposit different materials, resulting in layered structures. The technique offers high control over the mean thickness of the material deposited and it is a relatively fast process (in total about 2 $hours$ for each deposition, including pump time). The (nano)structure and roughness of the film depends on the material deposited and for thin films

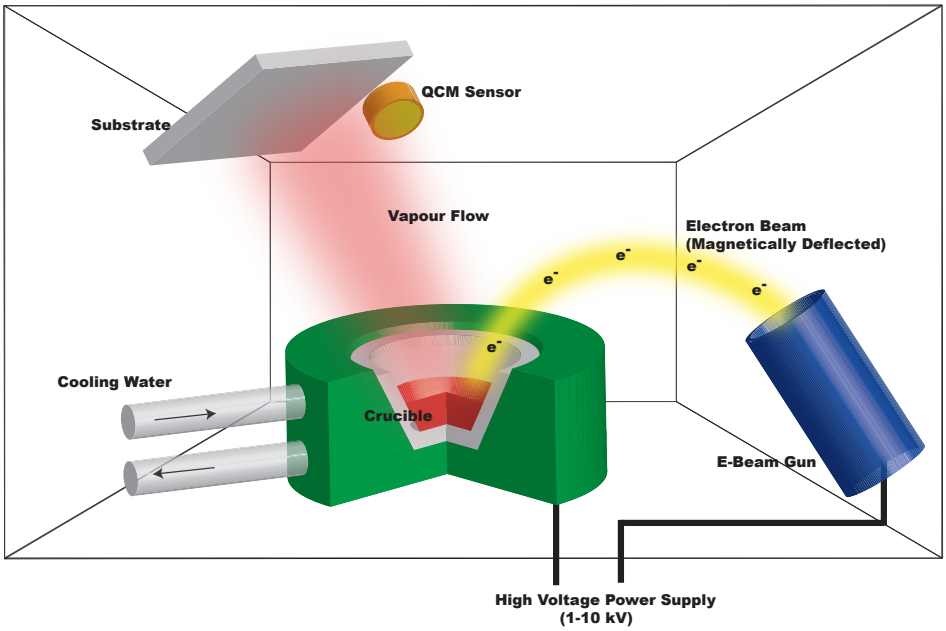

Figure 5.1: Schematic illustration of electron beam evaporation in vacuum used to manufacture all samples in paper I-III.

($< 20\ nm$) it is also highly dependent on the substrate. If the deposited material wets the substrate well, a continuous film is produced already at low mean thicknesses, whereas a material with poor wetting on the substrate forms a discontinuous particle film up to higher mean thicknesses. The fundamental process for the film growth is, however, similar for most material and substrate combinations and a schematic of the process is shown in figure 5.2. The first step is adsorption at nucleation sites (typically defects and step edges) on the substrate. As more material is deposited the particles grow and at some point they will merge together (coalescence) and form a film, which will become thicker as more material is deposited.

The resulting film structure can not be controlled directly as it depends on material and substrate. However, by learning how different combinations of material and substrate affect film structure one can get some control, and if temperature of the substrate can be varied more control is available (not available in the present work).

For this work, it should be mentioned, that for some materials the surface morphology may change when the sample is placed in the fuel cell. When

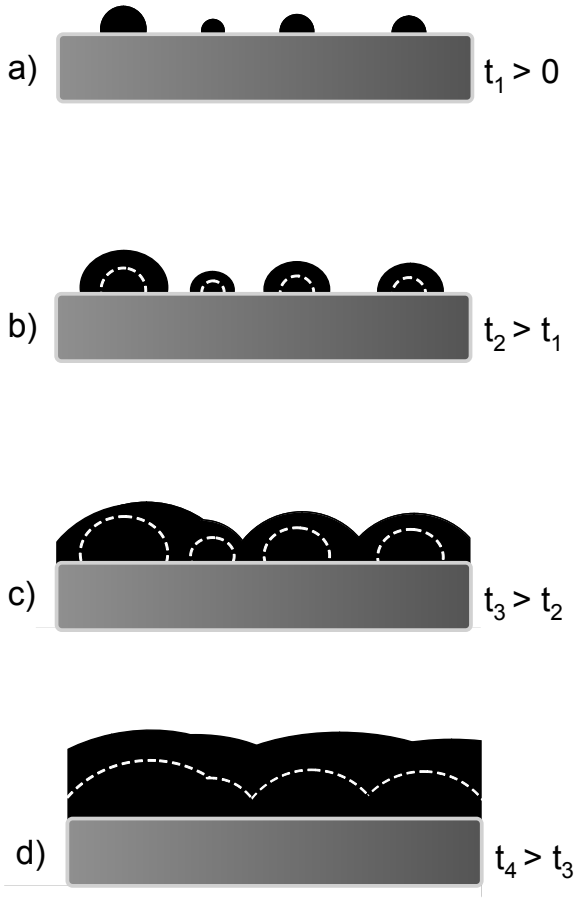

Figure 5.2: Schematic illustration of film growth in thermal evaporation, a) nucleation points, particle seeding, b) particle growth, c) particle coalescence, film formation and d) film growth.

possible, the samples should therefore be physically characterized both before and after fuel cell measurements. Below, the fabrication of the samples used in this work is explained in more detail and key features of the systems are discussed.

5.1.1 Sample fabrication on Nafion membranes

Before deposition, Nafion 117 membranes (purchased from Aldrich) where cleaned by sequential boiling in 3 % H_2O_2 for 1 h, 0.1 M H_2SO_4 for 1 h

and in three successive baths of Milli-Q water for 1 h each. The samples were then dried under flowing nitrogen gas. Prior to film deposition, the membrane surface was cleaned in mild oxygen plasma (PE/RIH, 50 W) for 2 min. The role of the oxygen plasma is to remove impurities, mainly hydrocarbons from the surface. This is important for sufficient adhesion. As oxygen plasmas are highly reactive it is assumed that it may also affects parts of the polymer membrane. In order to avoid membrane damage, mild (50 W) plasma conditions were used and proper function of the membranes was confirmed in fuel cell measurements.

Thin films were deposited onto the membranes in the vacuum system described above (AVAC). During deposition the membranes were in a dehydrated state, and the thin films adhered to the exposed Nafion polymer surface. A custom made holder was used to hold the flexible polymer membranes flat in position in the deposition chamber. The thin-film catalysts were later placed in a single cell fuel cell and used as cathode catalysts under realistic fuel cell conditions.

Simultaneous to the deposition on Nafion, thin films were also deposited on TEM windows [51] in order to facilitate examination of the nanostructure by transmission electron microscopy (TEM). For validation of this method, Nafion covered TEM-grids were used as substrates for control samples of 3 nm Pt films. Good agreement between the films deposited on Nafion and TEM windows was observed, and for practical reasons TEM windows were used as substrates for these sample types. Figure 5.3 shows TEM images of 3 nm of Pt, Au and TiO_2 (deposited as Ti and oxidized when exposed to air) deposited on TEM windows. As can be seen, the thin-film structure differs significantly between the materials. Ti has good wettability and the resulting structures are well spread out over the surface, whereas Au forms larger isolated particles and Pt forms a network structure. Although all samples have the same mean thickness, they correspond to different stages in the film growth mechanism, illustrated in figure 5.3.

In order for the model system to work properly as a fuel cell catalyst, it is vital that the catalyst layer is not so thick and/or dense that it blocks protons from reaching the membrane [50]. For most of the samples in paper I and II the thickness of the catalyst layer was chosen to be between 3 and 6 nm. However, in paper II, catalyst layers with thickness up to 21 nm were prepared.

Depositing material directly on membranes will create a good contact between catalyst and the proton conducting membrane. For the fuel cell to perform well there also has to be good contact between the catalyst and the electrode and at the same time there has to be enough porosity so that the reactant gas and the product water can be transported to and from the

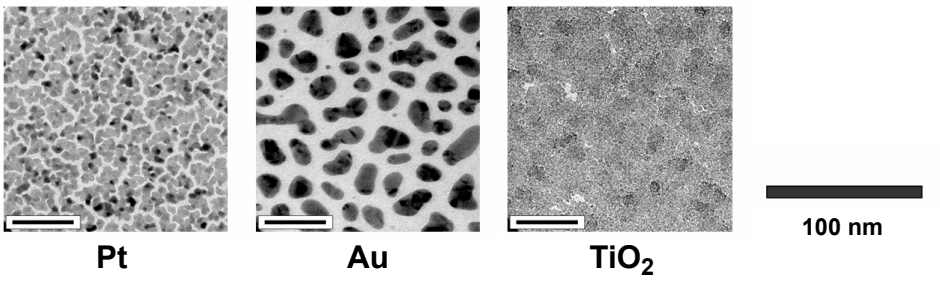

Figure 5.3: TEM images of thin films on TEM windows for 3 *nm* films (average thickness) of single materials, Pt, Au and TiO_2.

catalyst (the so called three phase boundary). From the electrochemical measurements it was seen that the mass activity of the thin films were significantly lower than what is seen in a conventional porous electrode at high current densities [52]. A reason for this can be a poor electric contact between the electrode and the thin catalyst layer. As the electrode is a porous structure it is likely that parts of the catalyst film will not be in contact with the electrode and thus not utilized in the measurements. The specific activity however, is as high or even higher for the samples with a thin catalyst layer deposited on membranes as compared to conventional electrodes [52].

In each sample series, the same type of electrodes and assembly procedure was employed and all electrochemical measurements were repeated with at least two separate samples for each sample type, with good agreement. Thus, the differences observed between different sample types have to be related to the structure and composition of the catalyst layers, which makes this model system suitable for qualitative comparison of catalyst materials.

5.1.2 Sample fabrication on gas diffusion layers

Deposition of catalyst directly on the gas diffusion layer (GDL) of a non-catalyzed electrode was done in paper III. In this case, all of the catalyst is in contact with the electrode and the catalyst-carbon interactions are similar to a conventional electrode. Deposition of the metal onto carbon instead of a membrane resulted in a different structure of the catalyst. Figure 5.4a shows SEM images of a Carbel Cl GDL before deposition and figure 5.4b shows the same GDL after deposition of 3 *nm* of Pt. As can be seen, Pt forms small particles of about $3 - 6$ *nm* in size on the exposed carbon particles. Since the electrode is porous, some of the deposited material will have little

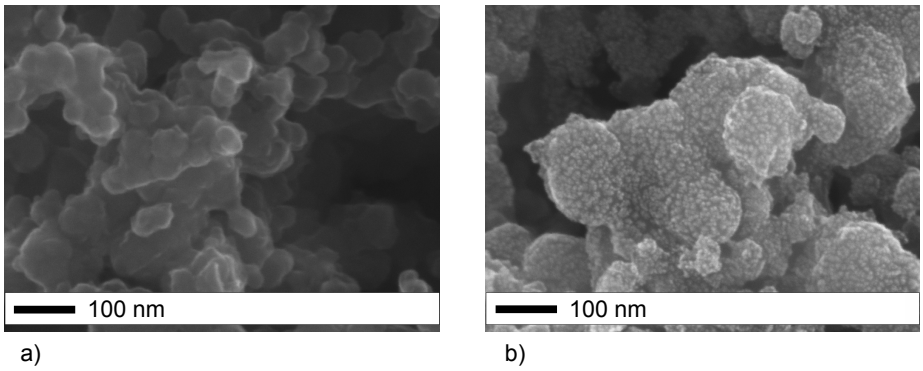

Figure 5.4: SEM micrograph of a) Carbel Cl prior to catalyst deposition and b) 3 nm Pt film on Carbel Cl.

or no contact with the membrane and hence, the proton conduction to the catalyst might be low in parts of the electrode. As for the system with catalyst deposited on membranes, this will result in a reduced use of catalyst material and a low mass activity is observed also for the system with catalyst on GDL compared to a conventional porous electrode.

A soft GDL (Carbel CL from Gore Technologies) and a hard GDL (Sigracet 34BC from SGL Technologies GmbH) have both been used as substrates for thin film deposition and have been electrochemically characterized. The harder GDL has the advantage that it can be disassembled from the MEA after fuel cell testing and physically characterized.

In this system, single Pt layers and multiple PtMe or $PtMeO_X$ layers have been studied. When incorporating a second material next to Pt, the effect on the catalyst structure has to be kept in mind. If the Pt is deposited on the GDL and the other material on top of Pt, it is likely that many Pt sites are blocked for reactant gases and/or protons from the ionomer. If it is placed between the Pt and the GDL it can affect the electric conduction and the structure of the Pt, since it is not evaporated on carbon.

5.2 Characterization methods

In this work, the characterization methods used can be divided in to physical and electrochemical methods. The physical methods were used to characterize the structure and composition of the samples. A range of electrochemical methods were employed to study the electrochemical behavior of the samples.

Most of the features seen in the electrochemical measurements are related to the structure and chemistry of the sample and it is thus important to use many techniques complementary. For example, the electrochemically measured surface area of the catalyst can be compared to microscopy images of the catalyst structure.

5.2.1 Physical methods

The thin film morphology was examined using scanning electron microscopy (SEM) and transmission electron microscopy (TEM). The chemical surface composition was determined by X-ray photoelectron spectroscopy (XPS) and X-ray diffraction (XRD) was used for crystallographic structure information.

For the thin films evaporated on membranes, characterization was made with SEM (JEOL JSM-6301F), XPS (Perklin Elmer PHI 5000C ESCA system) and fore some samples also with XRD (Siemens D5000 diffractometer). These measurements were done for films deposited on the same membranes as the ones that were tested in the fuel cell, and for some samples SEM characterization was also performed after they had been measured in the fuel cell. TEM (Phillips CM200) characterization was performed using TEM windows [51] as substrates.

TEM could not be used for characterization of the thin films evaporated on GDL. Instead High Resolution-SEM (Leo Ultra 55 FEG) was used to resolve the film structure.

5.2.2 Electrochemical methods

All samples were evaluated in a single cell PEM fuel cell (in cooperation with G. Lindbergh *et al.* at KTH). MEAs, with the thin-film catalyst as cathode was prepared by hot-pressing a GDL, a membrane and a commercial electrode (anode) at 135 ^oC for 30 s at 1 MPa. The MEAs were mounted in a homebuilt laboratory PEEK (polyether-etherketone) fuel cell, shown in figure 5.5 [53], in contact with circular 15 mm radius graphite current collectors with spirally formed gas channels. The cell was clamped together by applying a force of 380 N over the current collectors.

In the cell, the samples were evaluated using cyclic voltammetry (CV) in N_2 (inert atmosphere), CV in O_2 (polarization curves) and sometimes using high frequency impedance measurements. The CV in N_2 was in this work used to determine the active catalyst area and the influence of different material combinations on the electrochemical behavior of the catalysts. CV in O_2 gives the activity for ORR of the catalyst and measures the actual

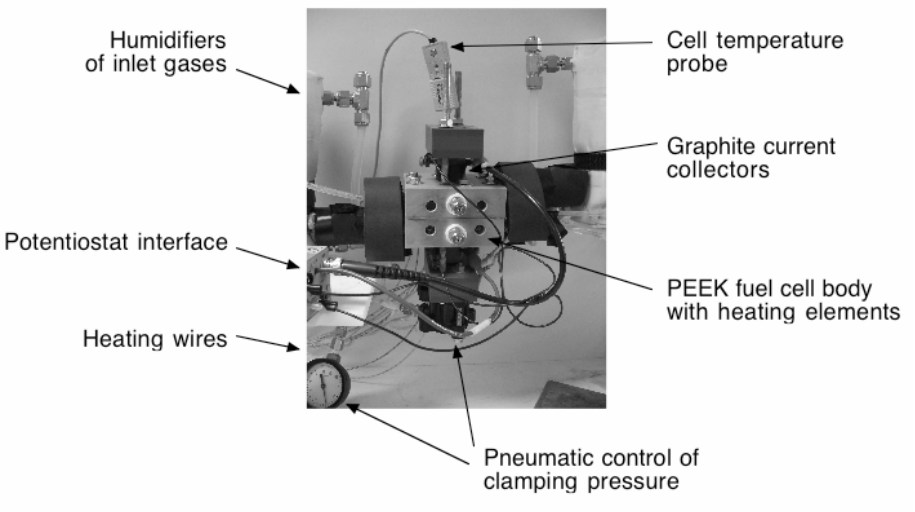

Figure 5.5: The single cell used for evaluation of the samples (Picture supplied by Henrik Ekström, KTH).

performance of the fuel cell. Impedance spectroscopy was in some cases used to measure the cell resistivity.

6

Summary of Results

This chapter discusses the background and scientific questions in each of the three papers. The main results are summarized and discussed in terms of their implications for practical systems and possible new questions and research opportunities that they raise.

6.1 Paper I

In paper I, the thin-film model system introduced in reference [49] was validated further. This was done by evaluating the ORR activity and electrochemical characteristics of thin films of Pt, Ir, Au and TiO_2. The results from polarization plots in oxygen and cyclic voltammograms in N_2 agree with previously reported data for these materials [54] and it was concluded that the thin-film model system can be used for ranking materials. Not surprisingly, the activity of the materials rank: Pt > Ir > Au >> TiO_2.

To investigate how Pt behaves in combination with other materials, bi-layered samples were fabricated using Pt in combination with Ir, Au or TiO_2. Moreover, the effect of deposition order was examined by making samples with Pt on top of or under the other material. All samples had a total thickness of 3 nm (1.5 nm of each material). For Au and Ir it was observed that the deposition order had little or no impact on the ORR activity. The Pt/Au system showed an increased activity compared to the sole Au sample but performed poorly compared to the pure Pt sample. The Pt/Ir system however, showed activities on the same order as the pure Pt sample although these samples only had half the amount of Pt. The addition of Ir also affected the voltammograms substantially where a large oxidation regime was noticed. The Pt/TiO_2 samples showed to differ in activity with respect to deposition order. TiO_2 on top of Pt showed less activity than the sample with Pt on top. Having Pt on top of TiO_2 resulted in almost the same activity as the pure Pt sample, where again the bi-layered sample only had half the amount

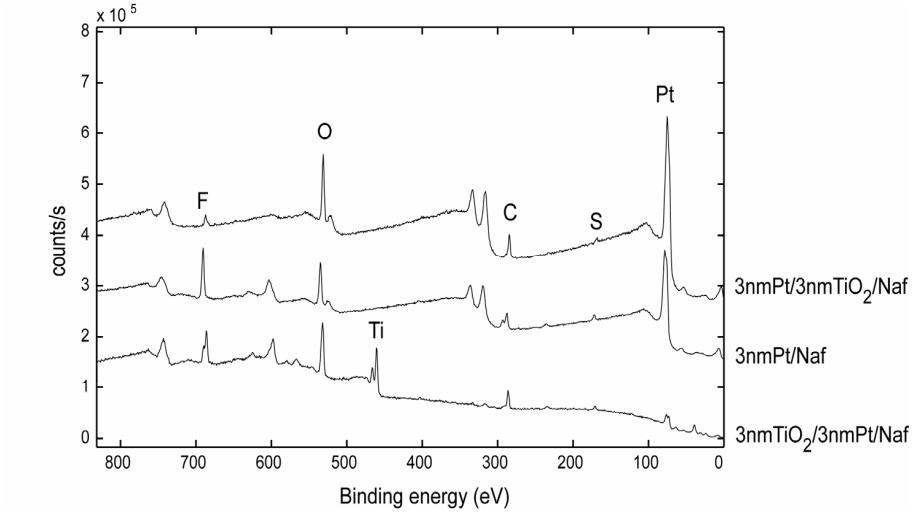

Figure 6.1: XPS analysis of thin films of Pt and TiO_2 deposited on Nafion with different deposition orders. Also, a pure Pt film is added for comparison.

of Pt. From the cyclic voltammograms it was seen that Pt on top of TiO_2 gave a higher available Pt area, something that might explain the higher ORR activity.

From XPS analysis it was concluded that the fabrication procedure gave a strongly layered structure as the top layer gave atomic concentrations of about $12 - 15$ % while the underlying material gave about $0 - 2$ %. This is also shown in figure 6.1 with XPS spectra for different deposition orders of Pt and TiO_2 (results not shown in paper I). TEM micrographs showed that the deposition order had a large effect on the resulting structure. However it should be pointed out that the TEM images were taken prior to the electrochemical evaluation and that it is possible that the material, at least for some material combinations, reorganized in the cell. Unfortunately it was not possible to perform the same characterization after the fuel cell measurements as the thin-film catalysts were hot pressed to the gas diffusion layer prior to mounting in the cell.

The electrochemical results led to speculations of the mechanisms involved in the relatively high activities seen for the Pt/Ir (both deposition orders) and the Pt/TiO_2 (especially Pt on top) samples. As deposition order did not affect the activity of the Pt/Ir samples and there where no clear indications of increased surface area of Pt it is likely that the mechanism

involved is a spill over effect between Ir and Pt. This can be explained by the fact that Ir has a lower oxidation potential than Pt and thus oxidizes easier. Other studies have identified the binding of OH and/or oxygen to Pt as being the rate limiting step in the ORR [28]. It is possible that in our system the presence of Ir can induce diffusion of OH and/or oxygen groups from Pt to Ir and thus free Pt sites. It is also possible that the mechanism is the reversed, that OH and/or oxygen is adsorbed on the Ir and then diffuse to the Pt where they are reduced to water.

As the voltammograms for the Pt/TiO_2 samples show a Pt like appearance, and the increased activity can be explained by the increased surface area when Pt is deposited on top of TiO_2 it was concluded that the TiO_2 acted as a stable and surface enhancing support rather than changing the kinetics of the process. The results were also seen as an indication of that TiO_2 can be a relatively good proton conductor over (at least) nanometer dimensions. This was studied further in paper II.

Pt/Ir and Pt/TiO_2 were also examined by making solid solution type (or mixed) samples by subsequently depositing 3 Å of Pt and Ir or Ti to a final thickness of 2.7 *nm* where the first and last layer was Pt. These samples however, showed poor ORR activity and high cell resistivities. One explanation for the poor performance can be increased mass-transport limitations for these samples. From TEM images it was seen that the mixed Pt/Ir and Pt/TiO_2 samples formed dense, well spread and homogenous layers, which can result in blocking of gas and proton transport through the thin layer. In particular for the Pt/TiO_2 mixed sample, it is interesting to note that the proton conduction of TiO_2 seems to be destroyed.

6.2 Paper II

Interesting properties of Pt in bi-layer combination with Ir and TiO_2 was observed in paper I and it was concluded that some Pt could be exchanged with Ir or TiO_2 without any loss of activity. For practical applications, Ir is not a good alternative to Pt as it is also a precious metal with a high price. TiO_2 on the other hand is a very cheap and abundant material and replacing some of the Pt with TiO_2 would lower the fuel cell cost substantially. Another observation from paper I is that the deposition order of Pt/Ti affected the activity for the ORR which the highest activity observed for Pt on top of TiO_2. In this configuration, the protons from the membrane have to diffuse through the TiO_2 layer to the Pt to react as it was concluded that TiO_2 in it self has no catalytic affect on the ORR.

In paper II, the effect of adding TiO_2 to the catalyst was further examined

and compared to that of oxides of Zr and Ta. All samples in this study had 3 nm of Pt on top of 1.5 nm of the additional metal which later oxidized to their natural oxides when the samples were vented to atmosphere. The metal oxides mainly functioned as a spacer layer for the electrolyte and catalyst. For TiO_2, spacer layers of up to 18 nm (of Ti) were fabricated to examine the proton conducting properties of TiO_2. This sample was compared with a thick layer of 20 nm of pure Pt, which should be very dense and thus have very low proton conduction. All samples were compared with a film of 3 nm Pt evaporated directly on the membrane without spacer layer, which served as a reference. The electrochemical characterization was performed in terms of oxygen reduction activity, high frequency impedance and cyclic voltammetry in N_2 in a fuel cell at 80 ^oC and full humidification.

Prior to the electrochemical measurements, the catalyst sample morphology and chemistry was examined using TEM, SEM and XPS. TEM analysis using TEM windows as in paper I showed that all samples with a metal oxide spacer layer had similar structures. The metal oxides readily wet the surface and create a high coverage film and the 3 nm film of Pt on top adapt to the structure of the metal oxide and is well distributed. The 3 nm Pt film without spacer layer form the same net-like structure as seen in paper I. The thick 20 nm Pt film showed a dense and fully covering film structure. Also in SEM all samples showed a similar and smooth structure. The SEM and XPS measurements were made on Nafion membranes, identical to the ones tested in the fuel cell. From the XPS characterization it was seen that the spacer layer metals were all in an oxidized state, with peak positions that correspond to TiO_2, ZrO_2 and Ta_2O_5 for Ti, Zr and Ta respectively. These are also the most stable oxides for the respective elements in the fuel cell environment.

Electrochemical characterization using high frequency impedance showed that the samples with ZrO_2 and Ta_2O_5 gave cell resistances $20 - 100$ times larger than for the pure 3 nm Pt sample or the 3 nm Pt on $1.5 - 18$ nm of TiO_2. The high resistance of the Zr and Ta samples also affected the voltammograms and gave them a tilted appearance. Consequently, the ORR activity measured in the polarization curves was poor for the Zr and Ta samples. Since the morphology of all samples was almost identical prior to the electrochemical measurements, the electrochemical differences have to be related to the materials and the processes in the fuel cell. High cell resistance is typically induced by poor proton conduction. As the metal oxides were observed to fully cover the membrane surface and protons have to be transferred through this layer to reach the catalyst, it is likely that it is this mechanism that was responsible for the increased cell resistance. Interestingly, TiO_2 even at a thickness of 18 nm gave no increase in resistance.

Evaporating thicker Ti films did not give reproducible results, probably since they do not completely oxidize to TiO_2 in the materials fabrication. The thick 20 nm Pt film rendered the highest cell resistance of all samples in this study, about 160 times higher than the 3 nm Pt and the 3 nm Pt on $1.5 - 18$ nm of TiO_2. The ORR activity for the 3 nm Pt on TiO_2 samples did not vary with thickness of the TiO_2 layer and was found to be approximately a factor of 2 higher than the pure 3 nm Pt film. The surface area of Pt, estimated from the cyclic voltammograms was substantially higher for the Pt on TiO_2 samples and did not vary with the oxide thickness.

After the fuel cell measurements, the MEAs were disassembled and the thin films characterized in SEM again. At this stage, all films showed a cracked, net-like structure, probably a result of membrane swelling/shrinking due to water uptake in the cell. Most importantly, the 3 nm Pt on 18 nm TiO_2 and the 20 nm Pt sample had very similar structure, with similar amount of cracks and dimensions. Thus, the proton conduction can not be explained by the protons moving in cracks in the film but have to be transported through the TiO_2 film.

To our knowledge, this is the first demonstration of proton conduction in TiO_2 measured in a fuel cell. However, there have been many reports on the proton conductivity of TiO_2 measured in other systems [55, 56, 57, 58]. The values of the conductivity depended on the preparation method and the observed differences are believed to be due to resulting differences in the structure of the TiO_2 layers. It is frequently reported that the conductivity of these materials is dependent on humidity since condensed water in the nanopores is believed to be involved in the proton conduction at high humidity [57, 58]. Some studies claim that the proton conduction of TiO_2 can surpass that of Nafion [55].

By fabricating thicker and more controlled TiO_2 layers, e.g. by anodic oxidation, and with the same measurement setup used in this work it would be possible to quantify the proton conductivity of TiO_2. This would be a very interesting study to perform as TiO_2 potentially has many advantages over Nafion, including a lower cost.

There are several possible mechanisms for the observed ion conduction in the TiO_2 films. One alternative is proton conduction ("as protons") through the bulk TiO_2, as reported by Lunell *et al.* [59] for anatase, or by the Grotthuss mechanism [58], occurring within hydrated nanopores in the TiO_2 film [57]. A combination of these two suggested mechanism may also be possible.

An important parameter in the proton conduction of TiO_2 is the crystal structure of TiO_2. Rutile is the thermodynamically most stable form for bulk TiO_2, but for nanostructures with a high surface area to volume ratio,

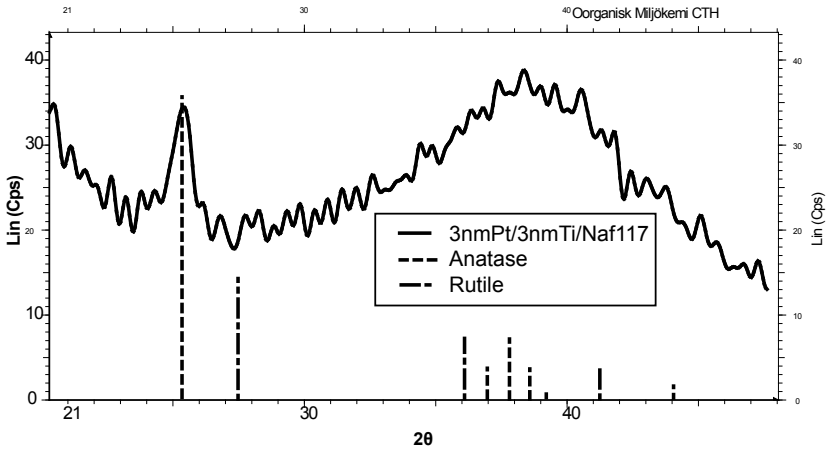

Figure 6.2: XRD spectra of a 3 nm Pt on 3 nm TiO_2 film on Nafion 117 membrane.

anatase is the most stable form [60]. To find the structure of the thin films used in this work, XRD measurements were performed. As seen in figure 6.2, anatase seems to be present, while no rutile is observed (results not showed in paper II). However, it should be mentioned that the XRD measurements gave a very weak signal and conclusions were hard to make. Since the amount of material in these samples is so low and further that the Nafion membrane is not flat on the mm range it is hard to probe the TiO_2. Another reason for the low XRD signal might be that the TiO_2 is mainly in a very microcrystalline to amorphous phase.

The findings in paper II proves that the proton conduction in TiO_2 is considerable over at least tens of nm, which potentially opens up for a number of applications of TiO_2 as electrolyte material in fuel cells. Areas of particular interest may be the application of TiO_2 in porous electrodes, as protective layer against fuel and oxygen permeation in various types of polymer fuel cells, or perhaps most intriguing; the usage of TiO_2 as the sole electrolyte in a proton exchange fuel cell.

6.3 Paper III

In paper III thin catalyst films were deposited on GDL rather than on membranes as in paper I and II. The reason for this was to explore how this

model system compared to the case when the catalyst is deposited on the membrane and to a conventional electrode. Another reason was to develop a model system in which the long-term stability of Pt in contact with carbon could be studied. It was seen that the degradation behavior of an evaporated Pt film on GDL is similar to that of a conventional electrode in terms of activity loss upon potential cycling. The effect of adding TiO_2 to the catalyst layer, both on the initial activity towards ORR and on the stability of the catalyst was studied electrochemically under realistic fuel cell conditions. Characterization prior to the fuel cell measurements was carried out using HR-SEM.

The samples discussed in paper III consisted of a pure 3 nm Pt film on GDL, 3 nm Pt on top of 10 nm TiO_2 on GDL and 10 nm of TiO_2 on top of Pt on GDL. Also a sandwiched sample with 10 nm of TiO_2 on both sides of a 3 nm Pt film on GDL was fabricated and tested (results not showed in paper III).

In the fuel cell, the samples were first tested for their activity for ORR and via cyclic voltammograms in N_2 in the same way as the samples in paper I and II. After this, an accelerated aging test consisting of excessive potential cycling was performed before the ORR activity and cyclic voltammetry was performed again to evaluate the effect of the corrosion test.

From the SEM characterization prior to the electrochemical measurements it was seen that Pt formed isolated particles about $3 - 6$ nm in size on carbon. This structure differs from the particle net-like structure seen on TEM windows in paper I and II. The reason for this is that differences in surface structure and surface properties between the TEM-window and the carbon particles results in the different film structures for the two supports. When Pt was deposited on top of TiO_2, no individual Pt particles could be seen, indicating that the Pt has a high wetting and is well spread.

Before the corrosion experiment, as seen in figure 6.3a and b, the pure Pt sample performed better than the TiO_2 containing samples. All samples had an almost identical surface area of Pt and it is reasonable to believe that the lower activity of the TiO_2 samples are related to *i*) poor electric conduction when TiO_2 is placed between the carbon and the Pt and *ii*) blocking of gases to Pt sites when TiO_2 is deposited on top of Pt. The sandwiched sample had the lowest ORR activity, probably as a result of both of these effects. After the corrosion experiments all samples lost a significant amount of Pt surface area, as seen in figure 6.3c and d, and showed a reduced ORR activity. Interestingly, the samples with Pt on top of TiO_2 corroded less than the samples when Pt was deposited directly on the carbon. The sample with 3 nm Pt on 10 nm TiO_2 now had the highest ORR activity, the pure Pt sample had a slightly higher activity than the sandwiched sample that in

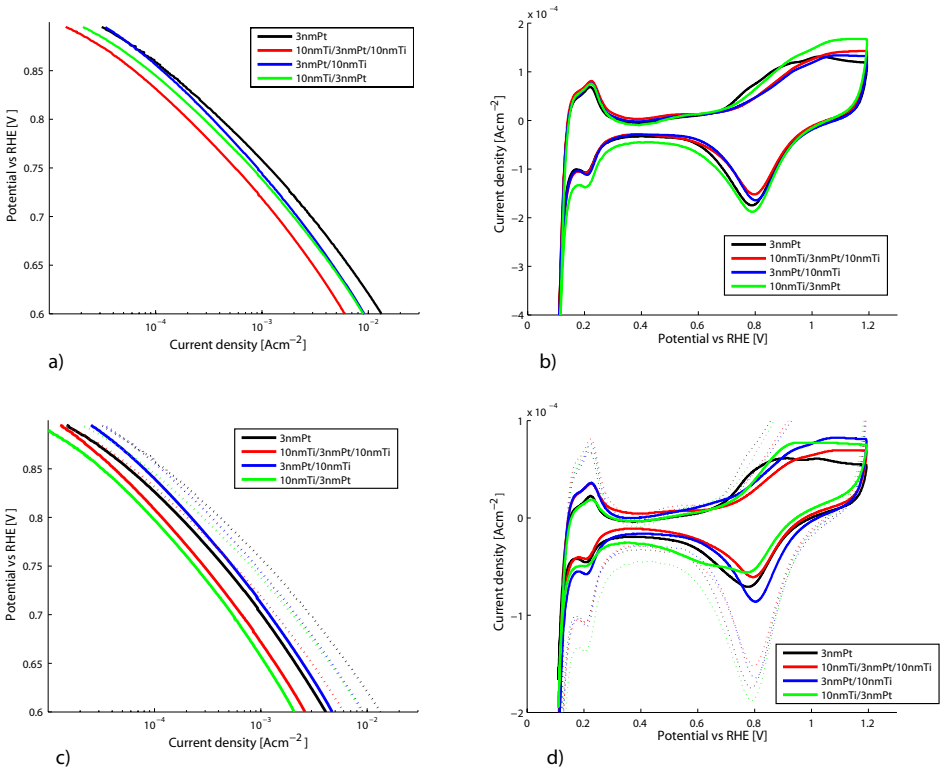

Figure 6.3: a) Polarization plot in oxygen before corrosion, b) Cyclic voltammetry in nitrogen before corrosion, c) Polarization plot in oxygen after corrosion and d) Cyclic voltammetry in nitrogen after corrosion for a pure 3 *nm* Pt film, 3 *nm* Pt film sandwiched between two 10 *nm* TiO_2 films, 3 *nm* Pt film on 10 *nm* TiO_2 and 10 *nm* TiO_2 on 3 *nm* Pt, all deposited on GDL.

turn performed better than the 10 *nm* TiO_2 on 3 *nm* Pt. The Pt surface area of the samples with Pt on carbon was similar for the two, and lower than that of the other two samples with Pt on TiO_2. Thus it seems that samples with Pt on TiO_2 had lost less surface area compared to the samples where Pt was in contact with carbon. The differences were small but they indicate the possibility that stabilizing Pt with other metals/materials may be possible.

7

Outlook

Model systems are a powerful tool to study central and basic properties and phenomena, and it has been demonstrated that they can be of great value for understanding and improving fuel cells. In the continuing work, I plan to further develop the model system fabrication, the electrochemical evaluation routines and include new characterization methods. More traditional model systems on planar supports with new nanofabrication procedures are presently being developed and preliminary results are promising. However, it is important to be able to measure model systems in realistic fuel cell environments. To include more detailed mechanistic studies, half cell experiments will be conducted as well as fuel cell measurements. Below follows a description of the electrochemical measurement setups that currently are being assembled.

7.1 Ongoing work

7.1.1 Single cell fuel cell

A single cell fuel cell, humidifiers, temperature regulators, mass flow controllers (MFCs), a three electrode potentiostat and a computer have been purchased. Figure 7.1 shows a photograph of the setup. The temperature regulators individually control the temperature of *i*) the cell, *ii*) anode humidifier, *iii*) cathode humidifier, *iv*) anode gas line between humidifier and cell and *v*) cathode gas line between humidifier and cell. The MFCs supply different gases or gas mixtures to the cathode and anode. Both the temperature regulators and the MFCs are controlled via a LabVIEW interface on the computer. The computer also controls the potentiostat via open source software. Different electrochemical measurements can be scripted sequentially in potentiostat software that has also been modified to communicate with the LabVIEW program. By doing this, it is possible to completely automate

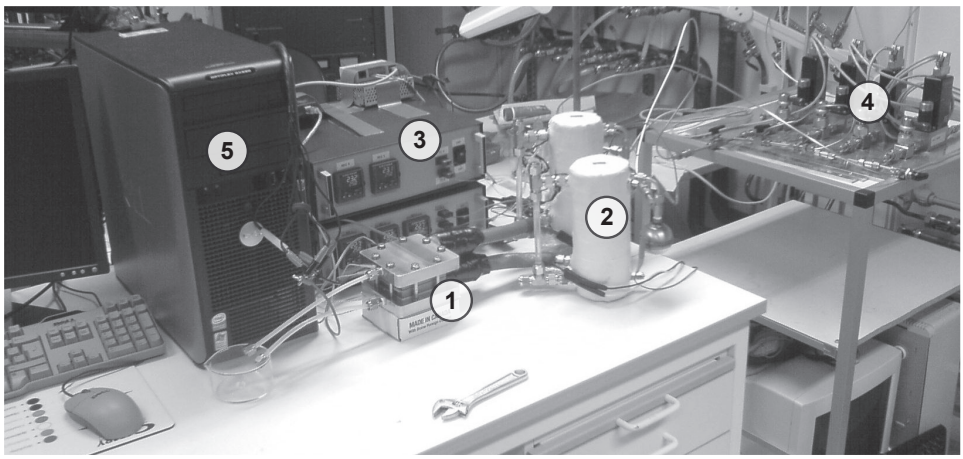

Figure 7.1: A photograph of the single cell fuel cell setup, 1) fuel cell, 2) humidifiers, 3) temperature regulators, 4) MFCs and 5) computer with potentiostat.

the measurements. Since a typical measurement in a fuel cell requires multiple electrochemical experiments with different gases and range from about $15 - 60\ h$ of measurement time, the automation of the test setup minimizes waiting times and allows overall faster characterization times. Moreover, the automation eliminates the risk of human errors in the measurement protocol.

At the moment the setup is assembled and initial benchmark tests have been performed. In the future this system will be used for the same types of electrochemical measurements as has been presented in this thesis. Moreover, the setup also has the possibility to supply CO to the fuel cell which can be used to determine the active catalyst area and to study CO oxidation, e.g. for anode catalysts.

7.1.2 EQCM

Electrochemical quartz crystal microbalance (EQCM) offers electrochemical half cell experiments in liquid electrolyte and at the same time monitor the mass change on the electrode surface. The concept has been described in literature [61, 62]. The quartz crystal sensor functions as the working electrode for the electrochemical measurements, and there is in addition a reference electrode located in the chamber and a counter electrode. Photographs of the EQCM cell is showed in figure 7.2. The mass sensitivity of the EQCM technique is about 0.5 ng/cm^2 which makes it possible to observe e.g. Pt

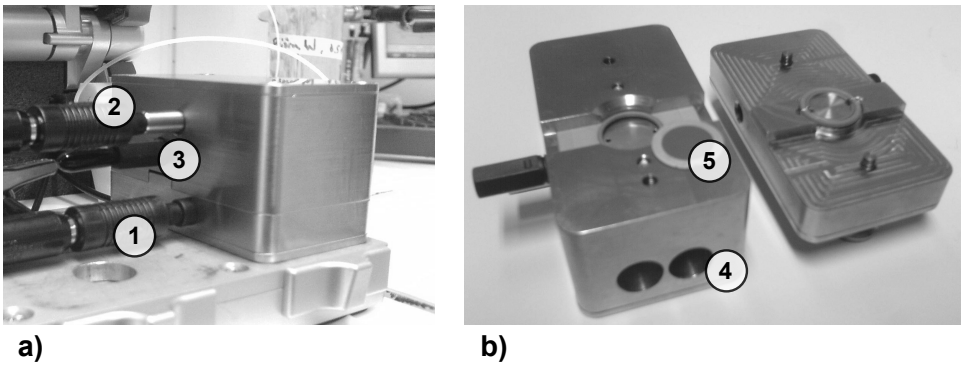

Figure 7.2: Photographs of the EQCM cell, 1) working electrode connected to the quartz crystal, 2) counter electrode, 3) reference electrode, 4) electrolyte flow channels and 5) a quartz crystal.

oxidation in a CV experiment on a flat Pt film. The EQCM technique is also ideal for studying stability of catalyst materials under electrochemical experiments. The high sensitivity of the EQCM in combination with nanofabrication makes it possible to perform mechanistic studies and make quantitative estimates of electrochemical and physical processes.

Initial tests have been performed and validated with experiments from literature with positive results. Figure 2.3 was measured using the EQCM setup. This setup will be used as a complement to the single cell setup and studies of catalyst stability have been planned.

7.2 Visions

A large technical barrier for the fuel cell commercialization is the short lifetime of the MEAs, related to catalyst and membrane degradation. This will be the main focus of the next coming studies and will involve both the single cell measurements and the EQCM.

It is also of great interest to increase the ORR activity and the utilization of Pt to reduce the cost of fuel cell systems. In order to do this improved understanding of Pt and Pt in contact with other materials is needed. Plans exist for preparing different types of nanostructures to help in these matters.

The fuel cell technology might be within reach and in a near future it is possible that a large number of applications are going to rely on fuel cells for energy conversion. If this will happen, to what extent and when is still to be seen and will depend on current and future research. I believe that fuel cells

will play an important role in tomorrow's society and my future work will be devoted to improve the fuel cell technology and assist its development.

Acknowledgements

First, I want to thank Prof Bengt Kasemo and Prof Magnus Skoglundh for giving me the opportunity to work at Chemical Physics and the Competence Centre for Catalysis (KCK).

An especially warm acknowledgement goes out to my supervisor, Dr Per Hanarp, for introducing me to the field of fuel cells and the practical work of nanofabrication. Thank you for all the time and effort you have invested and for pushing me in the right directions. None of this would have been possible without you.

My main supervisor, Docent Henrik Grönbeck is gratefully acknowledged. Your ability to capture the essence of a problem combined with vast expertise is a great source of motivation. Thank you for all the help in putting science in to words.

A key element in this work is the fruitful collaboration with my colleagues at KTH, for bringing the electrochemical expertise. A special thanks to Dr Henrik Ekström who have patiently performed measurements on my samples and educated me in electrochemistry.

The financial support of the Swedish Foundation for Environmental Research (MISTRA) as well as Autobrane (a part of the 6^{th} Framework Programme of the European Union) is gratefully acknowledged.

This work has been performed within the Competence Centre for Catalysis, which is hosted by Chalmers University of Technology and financially supported by the Swedish Energy Agency and the member companies: AB Volvo, Volvo Car Corporation, Scania CV AB, GM Powertrain Sweden AB, Haldor Topsøe A/S and The Swedish Space Agency.

I would like to thank all the people at Chemical Physics and the Competence Centre for Catalysis for showing me practical tips and tricks, creating an exciting atmosphere and good times. Hans Fredriksson for helping me with nanofabrication and proof reading and Andreas Lundström for excellent typesetting, deserve special credit.

Most importantly, my friends and family deserves all the gratitude for supporting me and keeping me close to the real world. Thank you all.

Bibliography

[1] Bierbaum, R. M., Holdren, J. P., MacCracken, M. C., Moss, R. H., and Raven, P. H. *Confronting Climate Change: Avoiding the Unmanageable and Managing the Unavoidable*. United Nations (Available from: http://www.unfoundation.org), (2007).

[2] *KEY WORLD ENERGY STATISTICS 2007*. IEA (Available from: http://www.iea.org), (2007).

[3] Bentley, R. W., Mannan, S. A., and Wheeler, S. J. *Energy Policy* **35**(12), 6364–6382 (2007).

[4] *Energiläget 2006*. The Swedish Energy Agency (Available from: http://www.energimyndigheten.se), (2006).

[5] Larmine, J. and Dicks, A. *Fuel Cell Systems Explained*. John Wiley and Sons, West Sussex, 2 edition, (2006).

[6] Gasteiger, H. A., Kocha, S. S., Sompalli, B., and Wagner, F. T. *Applied Catalysis B: Environmental* **56**(1-2), 9–35 (2005).

[7] *Fuel Cell Stack Durability*. DOE (Available from: http://www.hydrogen.energy.gov), (2006).

[8] Grove, W. R. *London and Edinburgh Philosophical Magazine and Journal of Science* **14**, 127–131 (1839).

[9] Barbir, F. *PEM Fuel Cells: Theory and Practice*. Elsevier Academic Press, London, (2005).

[10] O'Hayre, R. P., Cha, S.-W., Colella, W., and Prinz, F. B. *Fuel cell fundamentals*. John Wiley and Sons, New York, (2006).

[11] Mueller-Langer, F., Tzimas, E., Kaltschmitt, M., and Peteves, S. *International Journal of Hydrogen Energy* **32**(16), 3797–3810 (2007).

[12] Barbir, F. *Solar Energy* **78**(5), 661–669 (2005).

[13] Ni, M., Leung, M. K. H., Leung, D. Y. C., and Sumathy, K. *Renewable and Sustainable Energy Reviews* **11**(3), 401–425 (2007).

[14] Utaka, T., Sekizawa, K., and Eguchi, K. *Applied Catalysis A: General* **194-195**, 21–26 (2000).

[15] Svensson, A., Moller-Holst, S., Glckner, R., and Maurstad, O. *Energy* **32**(4), 437–445 (2007).

[16] Eaves, S. and Eaves, J. *Journal of Power Sources* **130**(1-2), 208–212 (2004).

[17] Kreuer, K. D. *Solid State Ionics* **97**(1-4), 1–15 (1997).

[18] Jannasch, P. *Current Opinion in Colloid and Interface Science* **8**(1), 96–102 (2003).

[19] Jones, D. J. and Roziere, J. *Journal of Membrane Science* **185**(1), 41–58 (2001).

[20] Litster, S. and McLean, G. *Journal of Power Sources* **130**(1-2), 61–76 (2004).

[21] Hermann, A., Chaudhuri, T., and Spagnol, P. *International Journal of Hydrogen Energy* **30**(12), 1297–1302 (2005).

[22] Godat, J. and Marechal, F. *Journal of Power Sources* **118**(1-2), 411–423 (2003).

[23] Gasteiger, H. A., Panels, J. E., and Yan, S. G. *Journal of Power Sources* **127**(1-2), 162–171 (2004).

[24] Pletcher, D. *A first course in electrode processes.* The Electrochemical Consultancy, Hants, (1991).

[25] Hamann, C. H., Hamnett, A., and Vielstich, W. *Electrochemistry.* Wiley-VCH, Weinhein, (2004).

[26] Tremiliosi-Filho, G., Jerkiewicz, G., and Conway, B. E. *Langmuir* **8**(2), 658–667 (1992).

[27] Chorkendorff, I. and Niemantsverdriet, J. W. *Concepts of Modern Catalysis and Kinetics.* Wiley-VCH, Weinheim, (2003).

[28] Norskov, J. K., Rossmeisl, J., Logadottir, A., Lindqvist, L., Kitchin, J. R., Bligaard, T., and Jonsson, H. *J. Phys. Chem. B* **108**(46), 17886–17892 (2004).

[29] *2005 Road Map Achievements.* Ballard (Available from: http://www.ballard.com), (2005).

[30] Bett, J. A. S., Kinoshita, K., and Stonehart, P. *Journal of Catalysis* **41**(1), 124–133 (1976).

[31] Ferreira, P. J., la O, G. J., Shao-Horn, Y., Morgan, D., Makharia, R., Kocha, S., and Gasteiger, H. A. *Journal of The Electrochemical Society* **152**(11), A2256–A2271 (2005).

[32] Yu, P., Pemberton, M., and Plasse, P. *Journal of Power Sources* **144**(1), 11–20 (2005).

[33] Passalacqua, E., Antonucci, P. L., Vivaldi, M., Patti, A., Antonucci, V., Giordano, N., and Kinoshita, K. *Electrochimica Acta* **37**(15), 2725–2730 (1992).

[34] Roen, L. M., Paik, C. H., and Jarvi, T. D. *Electrochemical and Solid-State Letters* **7**(1), A19–A22 (2004).

[35] Ball, S. C., Hudson, S. L., Thompsett, D., and Theobald, B. *Journal of Power Sources* **171**(1), 18–25 (2007).

[36] Mitsushima, S., Kawahara, S., Ota, K.-i., and Kamiya, N. *Journal of The Electrochemical Society* **154**(2), B153–B158 (2007).

[37] Antolini, E., Salgado, J. R. C., and Gonzalez, E. R. *Journal of Power Sources* **160**(2), 957–968 (2006).

[38] Tang, H., Peikang, S., Jiang, S. P., Wang, F., and Pan, M. *Journal of Power Sources* **170**(1), 85–92 (2007).

[39] Wang, C.-H., Shih, H.-C., Tsai, Y.-T., Du, H.-Y., Chen, L.-C., and Chen, K.-H. *Electrochimica Acta* **52**(4), 1612–1617 (2006).

[40] Arico, A. S., Bruce, P., Scrosati, B., Tarascon, J.-M., and van Schalkwijk, W. *Nat Mater* **4**(5), 366–377 (2005).

[41] Debe, M. K., Schmoeckel, A. K., Vernstrom, G. D., and Atanasoski, R. *Journal of Power Sources* **161**(2), 1002–1011 (2006).

[42] Kinoshita, K. *Journal of The Electrochemical Society* **137**(3), 845–848 (1990).

[43] Borup, R. L., Davey, J. R., Garzon, F. H., Wood, D. L., and Inbody, M. A. *Journal of Power Sources* **163**(1), 76–81 (2006).

[44] Bhushan, B., editor. *Springer handbook of nanotechnology*. Springer-Verlag, Berlin, (2004).

[45] Gates, B. D., Xu, Q., Stewart, M., Ryan, D., Willson, C. G., and Whitesides, G. M. *Chem. Rev.* **105**(4), 1171–1196 (2005).

[46] Libuda, J., Schauermann, S., Laurin, M., Schalow, T., and Freund, H. J. *Monatshefte fr Chemie / Chemical Monthly* **136**(1), 59–75 (2005).

[47] Behm, R. J. and Jusys, Z. *Journal of Power Sources* **154**(2), 327–342 (2006).

[48] Cha, S. Y. and Lee, W. M. *Journal of The Electrochemical Society* **146**(11), 4055–4060 (1999).

[49] Gustavsson, M., Ekstrm, H., Hanarp, P., Eurenius, L., Lindbergh, G., Olsson, E., and Kasemo, B. *Journal of Power Sources* **163**, 671–678 (2007).

[50] O'Hayre, R., Lee, S.-J., Cha, S.-W., and Prinz, F. B. *Journal of Power Sources* **109**(2), 483–493 (2002).

[51] Grant, A. W., Hu, Q.-H., and Kasemo, B. *Nanotechnology* **15**, 1175–1181 (2004).

[52] Ekström, H. *Evaluating cathode catalysts in the polymer electrolyte fuel cell*. Royal Institute of Technology (Available from: http://urn.kb.se/resolve?urn=urn:nbn:se:kth:diva-4413), (2007).

[53] Ihonen, J., Jaouen, F., Lindbergh, G., and Sundholm, G. *Electrochimica Acta* **46**(19), 2899 (2001).

[54] Appleby, A. *Catalysis Reviews* **5**, 221–243 (1970).

[55] Kasuga, T. *Thin Solid Films* **496**(1), 141–145 (2006).

[56] G., G.-B., Kytin, V., Dittrich, T., and Bisquert, J. *Journal of Applied Physics* **94**(8), 5261–5264 (2003).

[57] Tejedor-Tejedor, M. I., Vichi, F. M., and Anderson, M. A. *Journal of Porous Materials* **12**(3), 201–214 (2005).

[58] Colomer, M. T. *Journal of the European Ceramic Society* **26**(7), 1231–1236 (2006).

[59] Lunell, S., Stashans, A., Ojamae, L., Lindstrom, H., and Hagfeldt, A. *J. Am. Chem. Soc.* **119**(31), 7374–7380 (1997).

[60] Ranade, M. R., Navrotsky, A., Zhang, H. Z., Banfield, J. F., Elder, S. H., Zaban, A., Borse, P. H., Kulkarni, S. K., Doran, G. S., and Whitfield, H. J. *Proceedings of the National Academy of Sciences* **99**(90002), 6476–6481 (2002).

[61] Dam, V. A. T. and de Bruijn, F. A. *Journal of The Electrochemical Society* **154**(5), B494–B499 (2007).

[62] Jerkiewicz, G., Vatankhah, G., Lessard, J., Soriaga, M. P., and Park, Y.-S. *Electrochimica Acta* **49**(9-10), 1451–1459 (2004).

PAPER I

PAPER II

PAPER III